Estimating Synaptic Parameters from Mean, Variance, and Covariance in Trains of Synaptic Responses

Volker Scheuss and Erwin Neher

Max-Plack-Institut für biophysikalische Chemie, Abteilung Membranbiophysik, D-37077 Göttingen, Germany

ABSTRACT   Fluctuation analysis of synaptic transmission using the variance–mean approach has been restricted in the past to steady-state responses. Here we extend this method to short repetitive trains of synaptic responses, during which the response amplitudes are not stationary. We consider intervals between trains, long enough so that the system is in the same average state at the beginning of each train. This allows analysis of ensemble means and variances for each response in a train separately. Thus, modifications in synaptic efficacy during short-term plasticity can be attributed to changes in synaptic parameters. In addition, we provide practical guidelines for the analysis of the covariance between successive responses in trains. Explicit algorithms to estimate synaptic parameters are derived and tested by Monte Carlo simulations on the basis of a binomial model of synaptic transmission, allowing for quantal variability, heterogeneity in the release probability, and postsynaptic receptor saturation and desensitization. We find that the combined analysis of variance and covariance is advantageous in yielding an estimate for the number of release sites, which is independent of heterogeneity in the release probability under certain conditions. Furthermore, it allows one to calculate the apparent quantal size for each response in a sequence of stimuli.

INTRODUCTION

In fluctuation analysis of synaptic transmission, an alternative approach to the classical histogram method emerged over the past decade, which is referred to as ensemble noise analysis (Clamann et al., 1989), multiple probability fluctuation analysis (Silver et al., 1998), or variance-mean analysis (Reid and Clements, 1999; Oleskevich et al., 2000). It was adapted to synaptic transmission from ion channel noise analysis (Sigworth, 1980) and is based on the model-independent determination of the mean and the variance of synaptic responses under a set of conditions that cover a suitable range of transmitter release probabilities. The obtained relationship between variance and mean is then compared to the relationship predicted by a statistical model of synaptic transmission to estimate synaptic parameters. The classical, simple binomial model predicts a parabolic variance–mean relationship. A detailed description and discussion of the method was provided by Clements and Silver (2000). So far, the variance-mean analysis has mainly been restricted to steady-state sequences recorded under a variety of conditions, resulting in a range of mean response sizes (Silver et al., 1998; Reid and Clements, 1999; Oleskevich et al., 2000). In addition, sequences of double pulses (Oleskevich et al., 2000) and long repetitive trains of stimuli have also been used (Clamann et al., 1989), but no analysis dedicated to such nonstationary cases was presented.

Here we describe methods for applying the variance–mean analysis to short trains of synaptic responses for studying the mechanisms underlying synaptic short-term plasticity. In addition, we introduce the analysis of the covariance between successive synaptic responses in practice, which was already discussed theoretically by Vere-Jones (1966) and Quastel (1997). The covariance approach has some advantages over the variance–mean analysis alone and provides additional information about synaptic parameters during short-term plastic changes.

Fluctuation or noise analysis of synaptic transmission dates back to Del Castillo and Katz (1954). They introduced the quantal theory and quantal analysis of synaptic transmission based on the observation that evoked postsynaptic responses in a muscle fiber vary randomly between integer multiples of the spontaneous miniature response. Their analysis was based on binomial statistics, including Poisson statistics as a limiting case, with three parameters determining the size of a stimulus-evoked response: the average response size of the quantal unit q, and the binomial parameters p and N (e.g., McLachlan, 1978). Although p is generally associated with the release probability of one quantal unit, the interpretation of N is still controversial. It is suggested to be the number of docking sites, the available number of docked vesicles, or the number of morphologically defined active zones (Korn et al., 1982; Redman, 1990; Walmsley, 1993; Oleskevich et al., 2000).

Quantal analysis is applied to determine the functional parameters of a given synapse and to correlate any modification of synaptic efficacy with a change in one or more of the three parameters. In the classical histogram approach, as many synaptic responses as possible are collected in an amplitude histogram, which is treated as a multimodal distribution, with each mode representing a different number of quanta released. Ideally, this requires the identification of peaks in the histogram at a spacing of one quantal unit. The latter can be measured independently by recording sponta-

neously occurring miniature events (for reviews, see Redman, 1990; Walmsley, 1993). Especially in the CNS, the histogram approach is often compromised due to the presence of factors that obscure the amplitude quantization, such as high quantal contents, strong quantal-size variability, and heterogeneity in the release probability.

Frerking and Wilson (1996) summarize the coefficients of variation (CV_q) of quantal size distributions from miniature EPSC recorded in different preparations to be in the range of 44–90%. Heterogeneity in the release probability has been reported for a number of synapses (Walmsley et al., 1988; Rosenmund et al., 1993; Dobrunz and Stevens, 1997; Murthy et al., 1997; Sakaba and Neher, 2001). The degree of heterogeneity expressed in terms of coefficient of variation (CV_{pp}) is in the range of 22–71% in synapses of group 1 muscle afferents onto spinocerebellar tract neurons (Walmsley et al., 1988) and >50% in hippocampal synapses (Murthy et al., 1997).

These findings can be accounted for by applying compound binomial, multinomial, and compound multinomial models in the quantal analysis (Redman, 1990; Walmsley, 1993; Silver et al., 1998). However, in the case of histograms simply lacking peaks, quantization is contentious in spite of sophisticated fitting or deconvolution algorithms. The advantage of the variance–mean analysis is that the fluctuations of synaptic responses under different conditions are first quantified in a model-independent way by the variance and mean. The simple binomial model of synaptic transmission predicts a parabolic variance–mean relationship. Extensions of the theory accounting for quantal size variability or heterogeneity in the release probability introduce certain distortions to the simple variance–mean parabola (Silver et al., 1998). Thus, by fitting the respective relationship, the data can be interpreted in a very comprehensible way. Furthermore, the variance–mean approach is less noise sensitive and provides more and more reliable information, because it integrates or combines the data of different recording conditions with different mean response size.

When the variance–mean analysis is restricted to steady-state data sequences recorded at various conditions, e.g., by varying the external Ca^{2+} concentration or by application of long stimulus trains at different frequencies (which leads to various steady states of depression), the data necessarily yield information about synaptic parameters in steady state only. Here we present how the variance–mean approach can be applied to short, repetitive trains of non-stationary responses to study transient changes in the synaptic parameters during synaptic short-term plasticity. In short trains of stimuli the mean response amplitude is usually different for each stimulus due to short-term synaptic plasticity, such as paired-pulse facilitation (PPF) and short-term depression (STD). Applying such trains of stimuli repetitively and allowing sufficient time for recovery in between trains, one

can assume that corresponding responses in different trains represent identical conditions.

For quantitative analysis of nonstationary data, we explicitly derive equations for estimating synaptic parameters on the basis of the classical binomial model of synaptic transmission. We assume N independent release sites, which are either empty or occupied by a release-competent vesicle. Thus, a release site is not necessarily equivalent to an active zone, which is rather considered to represent a small group of release sites. We adopt the concept suggested by Zucker (1989) and Quastel (1997) that the release probability consists of the product of the probability p_A that a vesicle is available at a release site and the output probability p_0 in case a vesicle is available for release. We allow for heterogeneity by considering a nonuniform output probability among release sites. Intra- and intersite quantal variability is taken into account. Distinguishing p_A and p_0 provides an interpretation of synaptic depression by vesicle depletion. Furthermore, it allows an interpretation of the covariance between successive synaptic responses by depletion as shown theoretically by Vere-Jones (1966) and Quastel (1997). Quastel (1997) also suggested postsynaptic effects to contribute to the covariance between successive synaptic responses in addition to depletion. We allow for such postsynaptic effects, e.g., due to postsynaptic receptor saturation or desensitization, in our interpretation of the covariance.

METHODS

All the presented equations are derived assuming a binomial model of synaptic transmission as discussed in the introduction, applying basic principles of statistics. For verifying the hypotheses and studying situations, which cannot be solved analytically, we performed Monte Carlo simulations. The routines for simulation and analysis were programmed in IGORPRO (Wavemetrix, Lake Oswego, OR) and carried out on PC computers.

Release from $N = 500$ release sites in response to trains of five stimuli was simulated. Any release site could be either in the occupied, release competent state or in the empty state. Spontaneous transitions between the states, i.e., refilling, undocking, or spontaneous release, were computed according to a first-order kinetic scheme assuming an infinite reserve pool, as shown in Fig. 1 A. In such a scheme, the transition rate constants are determined by the recovery-time constant and the fraction of occupied sites at dynamic equilibrium, for which we used the parameters reported and proposed for the calyx of Held synapse. These were 4 s (von Gersdorff et al., 1997) and 80% (Meyer, 1999), respectively. The transition probabilities and the simulation time-step size were chosen such that the probability for a forward and backward transition within the same simulation time step was less than 0.001. Between the five evoked responses of the train, a number of simulation steps equivalent to 10 ms was computed, and between trains, a larger number equivalent to 10 s. Trains were repeated 10,000 times.

For evoked responses, an output probability was assigned to each release site. In the homogeneous case, this was the same for all sites. Heterogeneity was introduced by dividing the sites into two groups of 250 each, and assigning different output probabilities to the two groups. Evoked release was simulated by generating a random number distributed evenly in the interval [0, 1] for each release site in the occupied state and
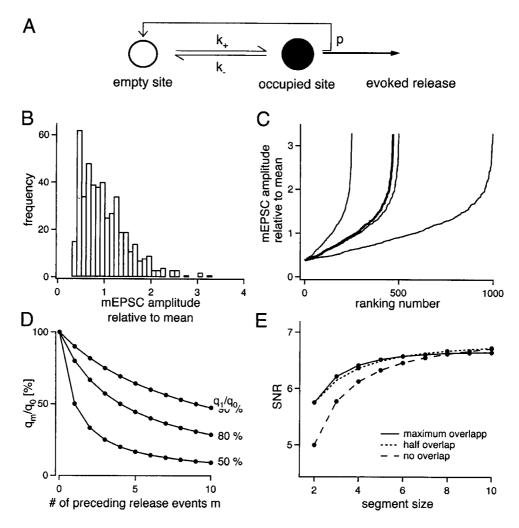
FIGURE 1   Simulation and analysis of synaptic transmission. (*A*) Kinetic scheme applied for the spontaneous release site transitions between the empty and the occupied, release competent state. (*B*) Histogram of the miniature EPSC data from the calyx of Held, which was used to generate ranked quantal-size data sets for the simulations. The CV_q is 0.5. (*C*) Ranked quantal-size data sets of different size (250, 469, 500, 1000), the bold line represents the ranked original data set. (*D*) Simulated quantal size reduction (Eq. 1) in terms of quantal size ratio q_m/q_0 depending on the number *m* of preceding release events if the quantal size ratio q_1/q_0 after a single release event is 90, 80, or 50% as indicated on the right. (*E*) SNR for the segment-wise variance estimation as described in Methods, plotted as a function of the segment size for a data set containing 100 samples: Independent, nonoverlapping segments (*broken line*); half-overlapping segments (*dotted line*); and completely overlapping segments (*line*). The dots mark the segment sizes, which are eligible in the respective approach.

comparing this number to the output probability assigned to that site. If the random number was smaller, a release event took place, the site was set to the empty state, and the size of the quantal response was determined as described below.

The quantal size assigned to individual release events was derived from miniature excitatory postsynaptic current (mEPSC) amplitude data recorded in the calyx of Held synapse, a histogram of which is shown in Fig. 1 *B*. The amplitude data was sorted according to increasing size and scaled such that the mean quantal size was equal to 1 in arbitrary units. The ranking numbers of the sorted data were used for assigning a quantal size to release events. Ranking number sets of a certain size were generated by extending or compressing the sorted amplitude data versus ranking number by interpolation, as shown in Fig. 1 *C*. In the case of intrasite quantal variability, a random number between 0 and 999 was generated and the corresponding quantal size chosen from a data set with 1000 ranking numbers. For intersite quantal variability, each of the 500 release sites was assigned a quantal size from a data set with 500 ranking numbers. In the

case of two groups of 250 sites, each of the 250 release sites was assigned a quantal size from a separate data set with 250 ranking numbers in order not to introduce correlation between release probability and quantal size.

A quantal size reduction during a train depending on the number of previous release events was implemented by a simplified empirical desensitization scheme. The quantal size is proportional to the number of open channels, which is reduced in case of desensitization. We assume a kinetic scheme such that channels enter the desensitized state from a transmitter-bound state, which does not necessarily have to be an open state, and further that equilibration of transmitter and receptor channels is faster than the transition to desensitization. Then one simply gets for the ratio of the reduced quantal size over the unperturbed quantal size in dependence on the number of previous release events *m* from the law of mass action

$$\frac{q_m}{q_0} = \frac{1}{1 + D \cdot m}. \tag{1}$$

Here D is defined by the quantal size ratio in the case of a single prior release event via $D \equiv q_0/q_1 - 1$, and m is limited by the number of postsynaptically interacting sites, denoted M in the simulations presented in Fig. 4. The relationship between the quantal size ratio and the number of preceding release events is shown in Fig. 1 D for a range of q_1/q_0 ratios. Assuming that stimuli occur faster than recovery from desensitisation ($\tau_{\text{recov}} = 19$ ms, Trussell et al., 1993), all preceding events were treated to contribute equally.

For the practical analysis contamination of the variance and covariance estimates by drifts or trends in the recording due to rundown or any other instability has to be minimized. Clamann et al. (1989) and Quastel (1997) suggested determination of mean, variance, and covariance by calculating these parameters over short segments or groups of sequential records and averaging the obtained values to give the overall or grand values of the parameter. There are several possibilities for dividing data into segments, such as nonoverlapping independent segments, half-overlapping and maximally overlapping segments. We calculated the accuracy of the variance estimates using these three approaches as a function of segment and data set size to determine an optimal segment size (see the Appendix). The accuracy of all three approaches is shown in Fig. 1 E as signal-to-noise ratio (SNR) for $N = 100$ and segment sizes between 2 and 10. It is seen that SNR is higher for larger segment sizes. This is particularly apparent for nonoverlapping segments. Therefore, one would prefer large segment sizes for ideal data. However, long segments can be expected to be contaminated by long-term trends more severely than short segments. Thus, there is a trade-off between potentially better SNR with larger signals and sensitivity to nonstationarities. We decided to use maximally overlapping segments of size two (Clamann et al., 1989, used independent segments of size 5 and 6), which yields the maximal suppression of contamination by long-term trends and drifts, but suffers only relatively little deficit in SNR compared to larger segments. For the covariance estimate, we calculated the accuracy for the condition of maximally overlapping segments of size 2, as presented in the Appendix.

Fits were performed with the built-in procedure of IGORPRO, based on minimization of χ^2. Fits to variance–mean plots were always weighted with the reciprocal of the standard deviation and constrained to pass the origin. If not otherwise stated results are reported as mean $\pm$ SEM.

THEORY AND RESULTS

Binomial model of synaptic transmission

Assume N release sites, which can be occupied by no more than one vesicle. Indexes x and y refer to release sites, indexes i and j to stimulus or response numbers. The model distinguishes between the all-or-none release process and the generation of the quantal postsynaptic response (considered here as a current; in the case of membrane potential, nonlinear summation might have to be considered). The all-or-none release process is associated with the parameter r with

$$r_{ix} = \begin{cases} 1 & \text{if release occurs at site } x \text{ in response to} \\ & \text{stimulus } i \\ 0 & \text{otherwise.} \end{cases} \quad (2)$$

Any given site is assumed to obey binomial statistics. The probability that a release event occurs at site x in response to stimulus i is the product of the probability $p_{\text{A}ix}$, that a vesicle is available at site x immediately before stimulus i, and the probability p_{0ix}, that an available vesicle is released from site x at stimulus i (Vere-Jones, 1966; Zucker, 1989; Quastel, 1997).

$$E(r_{ix}) = p(r_{ix} = 1) = p_{0ix}p_{\text{A}ix}, \quad (3)$$

$p_{\text{A}ix}$ and p_{0ix} are not assumed to be independent, see Eq. 19, Eq. 34 and following. Taking into account that the release probability is heterogeneous among release sites (Walmsley et al., 1988; Rosenmund et al., 1993; Murthy et al., 1997; Sakaba & Neher, 2001), the mean release probability over all release sites is $\langle p_{\text{A}i}p_{0i}\rangle$ with standard deviation σ_{pp} and coefficient of variation CV_{pp} ($\equiv \sigma/\text{mean}$), such that

$$\sum_{x=1}^{N} p_{\text{A}ix}p_{0ix} = N\langle p_{\text{A}i}p_{0i}\rangle \quad (4a)$$

$$\sum_{x=1}^{N} (p_{\text{A}ix}p_{0ix})^2 = N\sigma_{\text{pp}}^2 + \frac{1}{N}\left(\sum_{x=1}^{N} p_{\text{A}ix}p_{0ix}\right)^2$$

$$= N\langle p_{\text{A}i}p_{0i}\rangle^2(1 + \text{CV}_{\text{pp}}^2) \quad (4b)$$

In case an all-or-none release event occurs, the size of the quantal postsynaptic response q has some statistics associated to it, too. Intra- and intersite quantal variability can be distinguished (Frerking and Wilson, 1996). At a single release site x, the mean quantal size is $\langle q\rangle_{\text{Intra}}$, with standard deviation σ_{qIntra} and coefficient of variation $\text{CV}_{\text{qIntra}}$, such that

$$E(q_{ix}) = \langle q_{ix}\rangle_{\text{Intra}}, \quad (5a)$$

$$E(q_{ix}^2) = \sigma_{\text{qIntra}}^2 + E(q_{ix})^2 = \langle q_{ix}\rangle_{\text{Intra}}^2(1 + \text{CV}_{\text{qIntra}}^2). \quad (5b)$$

assuming that the intrasite quantal variability is the same at all sites, but not necessarily for all stimuli. Intersite quantal variability arises from the intrasite quantal size having different means among release sites. Intersite quantal variability with mean $\langle q\rangle_{\text{Inter}}$, standard deviation σ_{qInter}, and coefficient of variation $\text{CV}_{\text{qInter}}$ gives

$$\sum_{x=1}^{N} \langle q_{ix}\rangle_{\text{Intra}} = N\langle q_i\rangle_{\text{Inter}} \quad (6a)$$

$$\sum_{x=1}^{N} \langle q_{ix}\rangle_{\text{Intra}}^2 = N\sigma_{\text{qInter}}^2 + \frac{1}{N}\left(\sum_{x=1}^{N} \langle q_{ix}\rangle_{\text{Intra}}\right)^2$$

$$= N\langle q_i\rangle_{\text{Inter}}^2(1 + \text{CV}_{\text{qInter}}^2) \quad (6b)$$

$$\sum_{x=1}^{N} E(q_{ix})E(q_{jx}) = \frac{1}{N}\left(\sum_{x=1}^{N} \langle q_{ix}\rangle_{\text{Intra}}\right)\left(\sum_{x=1}^{N} \langle q_{jx}\rangle_{\text{Intra}}\right)$$

$$+ N\underbrace{\text{cov}(\langle q_{ix}\rangle_{\text{Intra}}, \langle q_{jx}\rangle_{\text{Intra}})}_{\leq \sigma_{\text{qInter}}^2} \quad (6c)$$

We follow the general assumption that release probability and mean quantal size are not correlated among release sites (but see Silver et al. 1998).

The EPSC recorded in response to stimulus i is the sum of the outputs over all release sites

$$I_i = \sum_{x=1}^{N} q_{ix} r_{ix}. \tag{7}$$

The mean EPSC amplitude I_i in response to stimulus i is the expectation of the sum in Eq. 7. With substitution of Eqs. 3, 5a and 6a this yields

$$\bar{I}_i = \sum_{x=1}^{N} \mathrm{E}(q_{ix} r_{ix}) = \sum_{x=1}^{N} \mathrm{E}(q_{ix}) \mathrm{E}(r_{ix})$$

$$= \sum_{x=1}^{N} \langle q_{ix} \rangle_{\mathrm{Intra}} p_{0ix} p_{Aix} = N \langle q \rangle_{\mathrm{Inter}} \langle p_{0i} p_{Ai} \rangle. \tag{8}$$

Variance and covariance are determined by the second moment. The second moment, M2, of the EPSC amplitude is

$$\mathrm{M2}_{ij} = E(I_i I_j) - E(I_i) E(I_j). \tag{9}$$

Substitution of Eq. 7 and 8 yields

$$\mathrm{M2}_{ij} = \sum_{x=1}^{N} \sum_{y=1}^{N} \mathrm{E}(q_{ix} r_{ix} q_{jy} r_{jy})$$

$$- \sum_{x=1}^{N} \sum_{y=1}^{N} \langle q_{ix} \rangle_{\mathrm{Intra}} p_{0ix} p_{Aix} \langle q_{jy} \rangle_{\mathrm{Intra}} p_{0jy} p_{Ajy} \tag{10}$$

Estimates for *N* and *q* from the variance–mean plot

The variance in the response amplitude at stimulus i is obtained by evaluating Eq. 10 for $i = j$. For the interpretation of the first expectation term $\mathrm{E}(q_{ix} r_{ix} q_{jy} r_{jy})$ in Eq. 10, different cases have to be distinguished. For the variance these are 1) Case one (release events occurring at the same site): $x = y$, $i = j$. Again with the assumption that release process and quantal size are independent, substitution of Eqs. 3 and 5b leads to

$$\mathrm{E}(q_{ix} r_{ix} q_{jy} r_{jy}) = \mathrm{E}(q_{ix}^2) E(r_{ix}^2)$$

$$= \langle q_{ix} \rangle_{\mathrm{Intra}}^2 (1 + \mathrm{CV}_{\mathrm{qIntra}}^2) p_{Axi} p_{0xi}. \tag{11}$$

2) Case two (release events occurring at separate sites): $x \neq y$; $i = j$. Again with the assumption of release site independence regarding the release process, independence of the release process and quantal size, and no interaction regarding the quantal size, (e.g., due to persistence of neurotransmitter in the synaptic cleft opposing an active zone or

spill-over on the time scale of release events), this is with substitution of Eqs. 3 and 5a,

$$\mathrm{E}(q_{ix} r_{ix} q_{jy} r_{jy}) = \mathrm{E}(q_{ix}) \mathrm{E}(r_{ix}) \mathrm{E}(q_{iy}) \mathrm{E}(r_{iy})$$

$$= \langle q_{ix} \rangle_{\mathrm{Intra}} \langle q_{iy} \rangle_{\mathrm{Intra}} p_{Aix} p_{0ix} p_{Aiy} p_{0iy}. \tag{12}$$

Substituting Eqs. 11 and 12 into Eq. 10 yields the variance,

$$\mathrm{Var}_i = \sum_{x=1}^{N} p_{Aix} p_{0ix} \langle q_{ix} \rangle_{\mathrm{Intra}}^2 (1 + \mathrm{CV}_{\mathrm{qIntra}}^2 - p_{Aix} p_{0ix}). \tag{13}$$

Based on the assumption that release probability and quantal size are not correlated, after insertion of Eq. 6b, it follows that

$$\mathrm{Var}_i = N \langle q_i \rangle_{\mathrm{Inter}}^2 (1 + \mathrm{CV}_{\mathrm{qInter}}^2)$$

$$\times ((1 + \mathrm{CV}_{\mathrm{qIntra}}^2) \langle p_{Ai} p_{0i} \rangle - (1 + \mathrm{CV}_{\mathrm{pp}}^2) \langle p_{Ai} p_{0i} \rangle^2). \tag{14}$$

Combining Eq. 8 and Eq. 14 yields the classical parabolic variance mean relationship in case that the quantal size is independent of the stimulus number, i.e. $\langle q_i \rangle_{\mathrm{Inter}} = q = $ const. (Sigworth, 1980; Silver et al., 1998)

$$\mathrm{Var}_i = q^* \bar{I}_i - \frac{1}{N_{\mathrm{var}}} \bar{I}_i^2, \tag{15}$$

and in the linear form (Heinemann and Conti, 1992),

$$\frac{\mathrm{Var}_i}{\bar{I}_i} = q^* - \frac{1}{N_{\mathrm{var}}} \bar{I}_i, \tag{16}$$

where the fitting parameters q^* and N_{Var} are related to the true parameters by

$$q = q^* (1 + \mathrm{CV}_{\mathrm{qIntra}}^2)^{-1} (1 + \mathrm{CV}_{\mathrm{qInter}}^2)^{-1}, \tag{17}$$

$$N = N_{\mathrm{Var}} (1 + \mathrm{CV}_{\mathrm{qInter}}^2)(1 + \mathrm{CV}_{\mathrm{pp}}^2). \tag{18}$$

Note that $\mathrm{CV}_{\mathrm{pp}}$ in Eq. 18 is not necessarily constant, but may be a function of the average release probability $\langle p_A p_0 \rangle$ (Quastel, 1997; Silver et al., 1998). The linear form in Eq. 16 has the advantage that procedures can be applied for weighted fitting, which consider uncertainties in both variables (Orear, 1982), to determine q^* and N_{var} from the y-axis intercept and the slope, respectively.

Estimating *N* and *q* from the covariance

The covariance in the response amplitudes at stimulus i and stimulus j is obtained by evaluating Eq. 10 for $i \neq j$. Regarding the first expectation term $\mathrm{E}(q_{ix} r_{ix} q_{jy} r_{jy})$ in Eq. 10, three cases have to be distinguished.

1) $x = y$. This considers previous and subsequent release from the same release site. Release occurring at both stimulus i and stimulus j requires that the release site is

reoccupied in between. Defining the probability of this reoccupation as $p_{Ai|jx}$ it follows, that

$$\mathrm{E}(r_{ix}r_{jx}) = p(r_{ix} = 1)p(r_{ix} = 1|r_{jx} = 1)$$

$$= p_{Aix}p_{0ix}p_{ai|jx}p_{0jx}. \quad (19)$$

In the framework of a vesicle pool model $p_{Ai|jx}$ can be expressed by the solution of the differential equations for vesicle recycling. For very simple models of recycling, it is given by $p_{Ai|jx} = p_{A1x}(1 - \exp(-\Delta t/\tau))$, where Δt is the inter-stimulus interval and τ the time constant of recovery (e.g., Weis et al., 1999). Furthermore, the quantal size of the subsequent release event might be affected by the previous release, e.g., due to desensitization or saturation. This is denoted by $q_{jx}(r_{ix})$ below. More accurately, this should also depend on how much was released previously, i.e. the quantal size q_{ix}. However, we assume that the variability in the neurotransmitter amount due to quantal size variability is negligible compared to the variability due to the fluctuation in the number of released vesicles. Then,

$$\mathrm{E}(q_{ix}r_{ix}q_{jx}r_{jx}) = \mathrm{E}(q_{ix})\mathrm{E}(q_{jx}(r_{ix}))\mathrm{E}(r_{ix}r_{jx})$$

$$= \mathrm{E}(q_{ix})\mathrm{E}(q_{jx}(r_{ix}))p(r_{ix} = 1)$$

$$\times p(r_{ix} = 1|r_{jx} = 1). \quad (20)$$

Substitution of Eqs. 3, 5a, and 19 yields

$$\mathrm{E}(q_{ix}r_{ix}q_{jx}r_{jx}) = \langle q_{ix}\rangle_{\mathrm{Intra}}\langle q_{jx}(r_{ix})\rangle_{\mathrm{Intra}}p_{Aix}p_{0ix}p_{Ai|jx}p_{0jx}. \quad (21)$$

2) $y \in [x - M/2, x + M/2]$. This considers release from any site to interact with previous release of its M neighbors, due to desensitization or saturation. The quantal size of the subsequent response depends on the previous release from the neighboring sites with $\mathrm{E}(r_{ix}q_{jy}) = \mathrm{cov}(r_{ix}, q_{jy}) + \mathrm{E}(r_{ix})\mathrm{E}(q_{jy})$. Thus,

$$\mathrm{E}(q_{ix}r_{ix}q_{jy}r_{jy}) = \mathrm{E}(q_{ix})\mathrm{E}(r_{ix}q_{jy})\mathrm{E}(r_{jy})$$

$$= \mathrm{E}(q_{ix})(\mathrm{cov}(r_{ix}, q_{jy}) + \mathrm{E}(r_{ix})\mathrm{E}(q_{jy}))\mathrm{E}(r_{jy}),$$

$$(22)$$

and substitution of Eqs. 3 and 5a yields

$$\mathrm{E}(q_{ix}r_{ix}q_{jy}r_{jy}) = \langle q_{ix}\rangle_{\mathrm{Intra}}(\mathrm{cov}(r_{ix}, q_{jy})$$

$$+ \langle q_{jy}\rangle_{\mathrm{Intra}}p_{Aix}p_{0ix})p_{Ajy}p_{0jy}. \quad (23)$$

3) $y \notin [x - M/2, x + M/2]$. In this case, there is no interaction between the sites. The expectation of the product is the product of the expectations. With Eqs. 3 and 5a, this gives

$$\mathrm{E}(q_{ix}r_{ix}q_{jy}r_{jy}) = \mathrm{E}(q_{ix})\mathrm{E}(r_{ix})\mathrm{E}(q_{jy})\mathrm{E}(r_{jy})$$

$$= \langle q_{ix}\rangle_{\mathrm{Intra}}\langle q_{jy}\rangle_{\mathrm{Intra}}p_{Aix}p_{0ix}p_{Ajy}p_{0jy}. \quad (24)$$

Inserting Eqs. 21, 23 and 24 into Eq. 10 and rearranging, the covariance between successive overall response amplitudes is

$$\mathrm{Cov}_{ij} = \sum_{x=1}^{N}(\mathrm{E}(q_{ix})\mathrm{E}(q_{jx}(r_{ix}))p_{Ai|jx}$$

$$- \mathrm{E}(q_{ix})\mathrm{E}(q_{ix})p_{Ajx})p_{Aix}p_{0ix}p_{0jx} \quad (25)$$

$$+ \sum_{x=1}^{N}\sum_{y=1}^{m}\mathrm{E}(q_{ix})\mathrm{cov}(r_{ix},q_{jy})p_{Ajy}p_{0jy}.$$

This equation is more complex and has not been discussed in the literature as much as the equation for the variance. Therefore the different aspects of the covariance analysis are considered separately in turn.

First it is assumed that there is effectively no refilling, i.e., $p_{Ai|jx} = 0$, which holds if the interstimulus intervals are brief enough. Furthermore, any effects of preceding release events on the subsequent quantal size are neglected, i.e., $\mathrm{cov}(r_{ix}, q_{jx}) = 0$, and the output probability is assumed to be homogenous, i.e., $\mathrm{CV}_{pp} = 0$. In this case of substitution of Eqs. 3, 5a, and 6c into Eq. 25 gives the covariance caused by vesicle depletion alone

$$\mathrm{Cov}_{ij}^{\mathrm{depl}} = -N\langle q_i\rangle_{\mathrm{Inter}}\langle q_j\rangle_{\mathrm{Inter}}(1 + \mathrm{CV}_{q\mathrm{Inter}}^2)p_{Ai}p_{0i}p_{Aj}p_{0j}$$

$$(26)$$

From this, N and quantal size q can be calculated as follows. Combining Eqs. 8 and 26 yields

$$N_{\mathrm{cov}} = -\frac{\bar{I}_i\bar{I}_j}{\mathrm{Cov}_{ij}^{\mathrm{depl}}}, \quad (27)$$

with $N = N_{\mathrm{cov}}(1 + \mathrm{CV}_{q\mathrm{Inter}}^2)$. The expression for N_{cov} including heterogeneity in the output probability is given in Eq. 32 for comparison to the estimate from the variance in Eq. 18. Combining Eqs. 8, 14, 17, and 26 gives

$$q_i^* = \frac{\mathrm{Var}_i}{\bar{I}_i} - \frac{\mathrm{Cov}_{i,i+1}^{\mathrm{depl}}}{\bar{I}_{i+1}} = \frac{\mathrm{Var}_i}{\bar{I}_i} - \frac{\mathrm{Cov}_{i,i-1}^{\mathrm{depl}}}{\bar{I}_{i-1}}, \quad (28)$$

with q^* as defined in Eq. 17. This allows the calculation of the quantal size for each response in a train separately, which is more specific than q^*, determined as a common parameter of all responses in the variance–mean parabola. (Note that there are two ways to calculate q. In practice, we take the average.)

The covariance gives a better estimate for *N* in case of *p* heterogeneity than does the variance–mean plot

Our simulations suggested (see below) that the covariance analysis gives a better N estimate than does the variance–

TABLE 1 Comparison of the *N* estimates from simulations

	CV$_p$	(1 + CV$_p^2$)	(1 + C$_{12}$)	Intrasite *q* variability		Intersite *q* variability	
				N/N$_{var}$	N/N$_{cov}$	N/N$_{var}$	N/N$_{cov}$
$\langle p_0 \rangle = 0.3$							
0.3	0.00	1.00	1.00	1.14	0.96	1.40	1.18
0.25/0.35	0.17	1.03	1.02	1.21	1.00	1.46	1.22
0.20/0.40	0.33	1.11	1.07	1.43	1.07	1.30	1.40
0.15/0.45	0.50	1.25	1.16	1.28	1.13	1.58	1.45
0.10/0.50	0.67	1.45	1.31	1.61	1.32	1.94	1.58
0.05/0.55	0.83	1.70	1.56	1.86	1.34	2.42	1.71
$\langle p_0 \rangle = 0.5$							
0.5	0.00	1.00	1.00	1.01	0.82	1.31	1.21
0.45/0.55	0.10	1.01	1.00	0.97	0.97	1.32	1.23
0.35/0.65	0.30	1.09	1.00	1.17	0.91	1.39	1.15
0.25/0.75	0.50	1.25	1.00	1.14	0.87	1.53	1.20
0.15/0.85	0.70	1.49	1.00	1.54	0.87	1.98	1.09
$\langle p_0 \rangle = 0.7$							
0.7	0.00	1.00	1.00	0.94	0.91	1.28	1.14
0.65/0.75	0.07	1.01	0.99	0.97	0.94	1.29	1.08
0.60/0.80	0.14	1.02	0.97	1.02	0.87	1.28	1.13
0.55/0.85	0.21	1.05	0.93	1.08	0.88	1.32	1.05
0.50/0.90	0.29	1.08	0.87	1.12	0.79	1.35	0.93
0.55/0.95	0.36	1.13	0.76	1.10	0.61	1.40	0.83

Values obtained from the variance–mean plot, as shown in Fig. 3, and by application of the covariance approach are shown.

The first column gives the output probabilities assigned to each of two groups of release sites for introducing heterogeneity for the three mean output probabilities considered: $\langle p_0 \rangle = 0.3$, 0.5, and 0.7 (see Methods for details).

The second to fourth columns show the resulting CV$_p$ and the correction factors $(1 + CV_p^2)$ and $(1 + CV_{1,2})$, respectively.

The last four columns summarize the ratios of the true number of sites over the estimates from the variance–mean plot and those obtained from the covariance approach. The two cases of intra- and intersite quantal size variability are compared. In each case the CV of quantal size variability was 0.5. According to Eqs. 18 and 32, the ratio N/N$_{var}$ (columns 5 and 7) should be identical to $(1 + CV_p^2)$ (column 3), considering, in the case of intersite quatal variability, the additional correction factor of $(1 + CV_{qInter}^2) = 1.25$. Likewise, the ratio N/N$_{cov}$ (columns 6 and 8) should be identical to $(1 + C_{12})$ (column 4). Given the number of repetitions in the simulation, the estimates should be accurate to about $\pm 10\%$, except for the case of N$_{cov}$, $\langle p_0 \rangle = 0.5$ and intersite quantal variability, for which the error is $\pm 20\%$.

mean parabola for mean output probability of $\langle p_0 \rangle = 0.5$ as documented in Table 1 and discussed below (see particularly Table 1, last line of the middle section in all cases the correct *N* value is 500). So the question arose whether it is a general feature that the covariance analysis is superior to the variance–mean parabola in the estimation of *N*, and why this might be the case. In the following analysis, it is again assumed that there is effectively no refilling, i.e., $p_{Ai|jx} = 0$. Furthermore, effects of preceding release events on the subsequent quantal size are neglected for simplicity, i.e., $\text{cov}(r_{ix}, q_{jx}) = 0$. In this case, Eq. 25 simplifies to

$$\text{Cov}_{ij}^{depl} = -\langle q_i \rangle_{\text{Inter}} \langle q_j \rangle_{\text{Inter}} (1 + CV_{qInter}^2)$$

$$\times \sum_{x=1}^{N} p_{Aix} p_{0ix} p_{Ajx} p_{0jx}. \qquad (29)$$

Combination of Eq. 8 with Eq. 29 and insertion of Eq. 4a yields

$$\frac{\text{Cov}_{ij}^{depl}}{\bar{I}_i \bar{I}_j} = -\frac{1}{N} \frac{\langle p_{Ai} p_{0i} p_{Aj} p_{0j} \rangle}{\langle p_{Ai} p_{0i} \rangle \langle p_{Aj} p_{0j} \rangle}$$

$$= -\frac{1}{N} (1 + C_{ij})(1 + CV_{qInter}^2), \qquad (30)$$

with

$$C_{ij} \equiv \frac{\text{cov}(p_{Ai} p_{0i}, p_{Aj} p_{0j})}{\langle p_{Ai} p_{0i} \rangle \langle p_{Aj} p_{0j} \rangle}, \qquad (31)$$

such that, because of Eq. 27,

$$N = N_{Cov} (1 + CV_{qInter}^2)(1 + C_{ij}). \qquad (32)$$

Comparing Eq. 32 to Eq. 18 yields an explanation for the question posed above by considering that $\sigma_{pp}^2 \geq \text{cov}(p_{Ai} p_{0i}, p_{Aj} p_{0j})$, see Eq. 4b for σ_{pp}. Thus one can argue that

$$C_{ij} = \frac{\text{cov}(p_{Ai} p_{0i}, p_{Aj} p_{0j})}{\langle p_{Ai} p_{0i} \rangle \langle p_{Aj} p_{0j} \rangle} \leq CV_{pp}^2. \qquad (33)$$

This means that the covariance can yield a better estimate for *N* than the variance–mean parabola. To analyze this further, the case $j = i + 1$ is considered. Because refilling is assumed to be negligible, p_{Ai+1} can be replaced by what remains after the previous response

$$p_{Ai+1} = p_{Ai}(1 - p_{0i}) \qquad (34)$$

and the evaluation of $C_{i,i+1}$ yields after some rearrangement

$$C_{i,i+1} = \frac{\langle p_{Ai}^2 \rangle (\langle p_{0i}p_{0i+1} \rangle - \langle p_{0i}^2 p_{0i+1} \rangle)}{\langle p_{Ai} \rangle^2 \langle p_{0i} \rangle (\langle p_{0i+1} \rangle - \langle p_{0i}p_{0i+1} \rangle)} - 1. \quad (35)$$

Assuming an initially uniform occupancy, i.e. $\langle p_{A1}^2 \rangle = \langle p_{A1} \rangle^2$, Eq. 35 yields

$$C_{1,2} = \frac{\langle p_{01}p_{02} \rangle - \langle p_{01}^2 p_{02} \rangle}{\langle p_{01} \rangle (\langle p_{02} \rangle - \langle p_{01}p_{02} \rangle)} - 1. \quad (36)$$

As a special case of heterogeneity in the output probability, we consider the situation (as assumed for the Monte Carlo simulations) with no facilitation ($p_{01} = p_{02} = p_0$) and two groups of equal numbers of release sites, one having an output probability of $p_0 = \langle p_0 \rangle - a$, and the other $p_0 = \langle p_0 \rangle + a$, with some parameter a ($\langle p_0 \rangle \geq a$), such that that $\langle p_0^2 \rangle = \langle p_0 \rangle^2 (1 + CV_p^2)$ and $\langle p_0^3 \rangle = \langle p_0 \rangle^3 (1 + 3CV_p^2)$. This yields

$$C_{1,2} = \frac{1 - 2\langle p_0 \rangle}{1 - \langle p_0 \rangle (1 + CV_p^2)} \cdot CV_p^2. \quad (37)$$

Thus the optimum condition, i.e., $C_{1,2} = 0$, for determining N from the covariance can readily be calculated in terms of mean output probability, which is $\langle p_0 \rangle = 0.5$. Furthermore, it holds that $(1 + C_{1,2}) < (1 + CV_p^2)$ unless CV_p approaches 1, as shown in Fig. 2 A (the case for two groups of release sites).

To evaluate $C_{1,2}$ for a more realistic p_0 distribution, we applied the beta distribution suggested by Silver et al. (1998), again assuming the case where $p_{01} = p_{02} = p_0$, and modeling the heterogeneity in p_0 according to a beta distribution. Note that Silver et al. (1998) used the beta distribution for the release probability, which we consider here as the product $p_A \cdot p_0$, i.e., of a probability of availability and an output probability. However, assuming that the availability is homogenous at the first stimulus, p_A can be considered as a scaling factor. p_0 is then distributed according to the beta distribution. The probability density function is

$$f(p_0) = \frac{1}{B(\alpha,\beta)} p_0^{\alpha-1}(1 - p_0)^{\beta-1}, \quad (38)$$
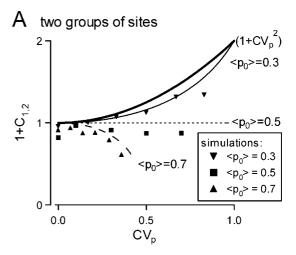
where $B(\alpha, \beta)$ designates the beta function. Evaluation of the nth moment yields

$$\langle p_0^n \rangle = \prod_{i=0}^{n-1} \frac{(\alpha + i)}{(\alpha + \beta + i)}, \quad (39)$$

Such that the parameters α and β are related to the mean and coefficient of variation of the p_0 distribution in the following way:

$$\alpha = 1 - (1/CV_p^2 + 1)\langle p_0 \rangle, \quad (40a)$$

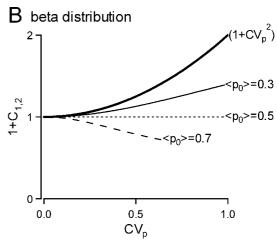$$\beta = (1/\langle p_0 \rangle - 1)\alpha. \quad (40b)$$

FIGURE 2 Correction factor $(1 + C_{1,2})$ for the estimate of N from the covariance in comparison to the correction factor $(1 + CV_p^2)$, which applies to the variance–mean plot (*heavy solid line*). $(1 + C_{1,2})$ is shown for mean output probabilities of $\langle p_0 \rangle = 0.3$, 0.5, and 0.7 versus the coefficient of variation CV_p ranging from 0 to 1. (*A*) $(1 + C_{1,2})$ in the case of two groups of release sites with different p_0 (*lines*, for details refer to text) and as obtained from the simulation shown in Fig. 3 and Table 1 regarding intrasite quantal variability (*symbols*). (*B*) $(1 + C_{1,2})$ in the event that p_0 is distributed according to a beta distribution.

Insertion of Eqs. 39 and 40 into Eq. 36 yields a complicated analytical expression, which is not explicitly given here. The calculated result is shown in Fig. 2 B, where $(1 + C_{1,2})$ is compared to $(1 + CV_p^2)$ for the beta distribution. Again, it is seen that the correction factor for N_{cov} is quite close to 1, even for large heterogeneity, if $\langle p_0 \rangle$ is close to 0.5.

Simulations with heterogeneity in the output probability

To compare the N estimates from the variance–mean plot (Eq. 15) with the estimate from the covariance (Eq. 27), simulations were carried out as described in the methods for $N = 500$ release sites with mean output probabilities $\langle p_0 \rangle$ of
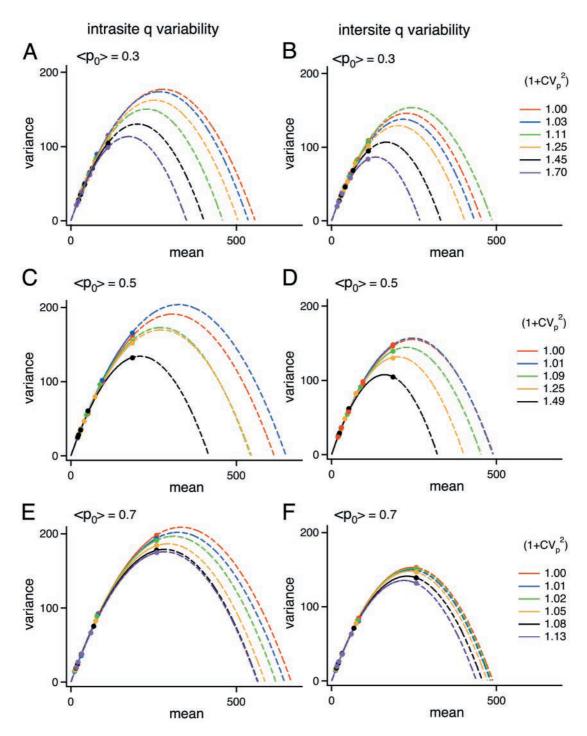
FIGURE 3   Variance–mean plots of simulated data. Simulations with $N = 500$ release sites, mean output probability of $\langle p_0 \rangle = 0.3$ (A, B), 0.5 (C, D), and 0.7 (E, F), and different degrees of heterogeneity are shown. The legend in panel B applies to the whole figure. Quantal size variability had a CV_q of 0.5 in each case. In the left column (A, C, E), the quantal size variability was assumed to be of the intrasite type. In the right column (B, D, F), the case intersite variability is shown. The theoretical correction factors for the N estimates from the variance–mean plot $(1 + CV_p^2)$ are given on the right-hand side to indicate the degree of heterogeneity. The N estimates obtained from the parabolic fits (N_{var}) are compared to the estimates from the covariance (N_{cov}) in Table 1. All data are shown in arbitrary units with respect to a quantal size of 1 unit.

0.3, 0.5, and 0.7 and different degrees of heterogeneity in the output probability. We also compared the effects of intra- and intersite quantal variability. The results are sum- marized in Figs. 2 and 3, and Table 1. In each case, a parabolic fit to the simulated data points is shown (Fig. 3). The degree of curvature in the variance–mean parabolas,

and, consequently, the N_{var} estimate is effectively determined by the first (largest!) response in the train. Later responses in the train lie on the linearly rising part of the parabolas, see Fig. 3. Intersite quantal variability generally leads to an underestimation of N, see Fig. 3, B, D, and F, and Table 1, as expected from Eqs. 18 and 32 with $CV_{qInter} = 0.5$ (note, that N/N_{var}-values and N/N_{cov}-values of Table 1 are systematically larger by a factor of $(1 + CV_{qInter}^2) \approx 1.25$ for the case of intersite quantal variability as compared to intrasite variability).

At low mean output probability, i.e., $\langle p_0 \rangle = 0.3$, the variance–mean parabola (Fig. 3, A and B) and the covariance approach (Table 1, top) both underestimate N with increasing p_0 heterogeneity to an extent accurately predicted by Eqs. 18 and 32 with the correction factors $(1 + CV_p^2)$ and $(1 + C_{1,2})$ as plotted in Fig. 2 A (*solid* and *thin lines*), respectively. The estimates from the covariance are acceptable for small degrees of heterogeneity. At medium mean output probability, i.e., $\langle p_0 \rangle = 0.5$, N_{cov} slightly overestimates N, but the estimates appear not to be affected by any degree of p_0 heterogeneity, because $(1 + C_{1,2}) \approx 1$, as expected from Eq. 37 (Fig. 2 A, *dotted line*). The variance–mean parabola, however, underestimates N with increasing heterogeneity (Fig. 3, C and D, Table 1, middle). At high mean output probability, i.e., $\langle p_0 \rangle = 0.7$, the variance–mean estimate is affected by increasing heterogeneity (Fig. 3, E and F), but less compared to the case of small mean output probability of $\langle p_0 \rangle = 0.3$ (Fig. 3, A and B). The reason for this is that the same degree of heterogeneity yields a lower CV_p at higher mean. The covariance approach considerably overestimates N at high $\langle p_0 \rangle$ (Table 1, bottom), as expected from Eq. 37 (Fig. 2 A, *broken line*). The analytically derived dependence of the correction factor $(1 + C_{i,i+1})$ for the N_{cov} estimates on the mean and degree of heterogeneity in the output probability in case of two groups of release sites (Eq. 37), is confirmed by our simulations. Figure 2 A shows good agreement between the analytical relationship (*lines*) and the values obtained for $(1 + C_{i,i+1})$ by dividing $N = 500$ by N_{cov} from the simulations (*symbols*; Eq. 32).

This shows that the covariance approach yields a good N estimate, which is unaffected by heterogeneity in the output probability under conditions with intermediate mean output probability, ideally $\langle p_0 \rangle = 0.5$. In the range between $\langle p_0 \rangle = 0.3$ and $\langle p_0 \rangle = 0.7$, the N_{cov} estimate is accurate within $\pm 40\%$ as long as $CV_p < 75\%$. The variance–mean plot provides reasonable N estimates for small degrees of heterogeneity under conditions of high mean output probability. However, both approaches suffer the same from the presence of intersite quantal variability as expected from Eqs. 18 and 32.

Effect of saturation and desensitization on the estimates from the covariance

It must be considered that correlation might not only arise from depletion of vesicles, but also from desensitization or saturation, in case of persistence of neurotransmitter in the synaptic cleft or spillover as a consequence of repetitive activity (Trussell et al., 1993; Otis et al., 1996a; Barbour and Häusser, 1997).

Here, it is again assumed that there is effectively no refilling, i.e., $p_{Ai|jx} = 0$. Effects of preceding release events on the subsequent quantal size are considered, i.e., $\text{cov}(r_{ix}, q_{jx}) \neq 0$, but quantal size variability and heterogeneity in the release probability are now neglected for simplicity. In this case, substitution of Eqs. 3 and 4a into Eq. 25 gives for the total covariance caused by depletion and postsynaptic effects,

$$\text{Cov}_{ij}^{total} = -Nq_i q_j p_{Ai} p_{0i} p_{0j}\left(1 - \frac{M\,\text{cov}(r_i, q_j)}{q_j p_{Ai} p_{0i}}\right)p_{Aj}, \quad (41)$$

where M is the number of postsynaptically interacting release sites, as detailed in the methods section. Comparing Eq. 41 and Eq. 26 (in the absence of quantal size variability, i.e., $CV_{qInter} = 0$), it is seen that the total covariance caused by depletion and postsynaptic effects can be expressed as the covariance caused by depletion alone (Cov_{ij}^{depl}) increased by a factor depending on the covariance caused by postsynaptic effects

$$\text{Cov}_{ij}^{total} = (1 - D_{ij})\text{Cov}_{ij}^{depl}, \quad (42)$$

with

$$D_{ij} \equiv \frac{M\,\text{cov}(r_i, q_j)}{q_j p_{Ai} p_{0i}}. \quad (43)$$

Below we will show that $D_{i,i+1}$ is always negative, if release leads to a decrease in quantal size, such that the correction factor $(1 - D_{i,i+1})$ represents, indeed, the sum of the covariance of presynaptic origin and that caused by postsynaptic effects.

Thus, for estimating N and q from the total covariance (Eq. 42) according to Eq. 27 and Eq. 28, the correction factor $(1 - D_{i,i+1})$ is introduced

$$N = -(1 - D_{i,i+1})\frac{\bar{I}_i \bar{I}_{i+1}}{\text{Cov}_{i,i+1}^{total}} = N_{Cov}(1 - D_{i,i+1}), \quad (44)$$

$$q_i = \frac{\text{Var}_i}{\bar{I}_i} - (1 - D_{i,i+1})^{-1}\frac{\text{Cov}_{i,i+1}^{total}}{\bar{I}_{i+1}}$$

$$= \frac{\text{Var}_i}{\bar{I}_i} - (1 - D_{i-1,i})^{-1}\frac{\text{Cov}_{i-1,i}^{total}}{\bar{I}_{i-1}}. \quad (45)$$

An interpretation of the term $\text{cov}(r_i, q_{i+1})$ and of D is obtained by using Eq. 3. Evaluating the mean quantal size of a subsequent response to be a weighted average of the cases with and without prior release, one obtains

$$D_{i,i+1} = \frac{E(r_i q_{i+1}) - E(r_i)E(q_{i+1})}{q_{i+1} p_{Ai} p_{0i}}. \quad (46)$$

The first expectation term in the numerator is $E(r_i q_{i+1}) = q_{i+1}(r_i = 1)p_{Ai}p_{0i}$, i.e., the quantal size resulting after a preceding release event times the probability of such an event. Further, with $E(q_j) = q_j$ under the condition considered here and Eq. 3, one obtains from Eq. 46,

$$D_{i,i+1} = M\left(\frac{q_{i+1}(r_i = 1) - q_{i+1}}{q_{i+1}}\right), \qquad (47)$$

such that $D_{i,i+1}$ is proportional to the number of interacting sites M and the change of the quantal size caused by a preceding release event, relative to the mean quantal size. Therefore, $D_{i,i+1}$ can be assumed to be largely independent of quantal-size variability and heterogeneity in the release probability, such that, in practice, $(1 - D_{i,i+1})$ can be considered as an additional, independent correction factor for the N_{cov} estimate (Eq. 32), to give

$$N = N_{Cov}(1 + CV_{qInter}^2)(1 + C_{i,i+1})(1 - D_{i,i+1}). \quad (48)$$

Similarly the quantal-size estimate from Eq. 45 can be considered to be q^* as defined in Eq. 17; i.e., it has to be corrected for quantal size variability to obtain the mean quantal size.

Evaluating the ratio of the correlation coefficient ρ_{ij} in the amplitude of successive responses, defined as $\rho_{ij} = Cov_{ij}/(Var_i \cdot Var_j)$, according to Eqs. 14 and 41, obtained under two recording conditions, which are equivalent except for the presence and absence of postsynaptic effects (e.g., by application of appropriate drugs), yields the correction factor $(1 - D_{ij})$ as

$$(1 - D_{ij}) = \rho_{ij}(control)/\rho_{ij}(drug). \qquad (49)$$

Simulations with desensitization

To study the effect of correlation due to modulation of the quantal size by preceding release events on the estimates from the covariance, we chose, as an example, postsynaptic receptor desensitization for Monte Carlo simulations. Simulations were carried out as described in the methods for $N = 500$ release sites, a homogenous output probability of $p_0 = 0.5$, and a quantal size reduction according to Eq. 1. First simulations with $M = 3$ interacting sites, together with a reduction of quantal size by a single preceding release event to $q_1/q_0 = 80\%$ and 50%, were performed. As a second example $M = 20$ together with $q_1/q_0 = 90\%$ and 80% was used. The case $M = 3$ is thought to represent the situation of the local postsynaptic interaction of release events at an active zone, whereas $M = 20$ considers more global postsynaptic interaction of release events by spillover. One set of simulations was generated with intrasite quantal variability and another one with intersite quantal variability.

There was no obvious difference between intra- and intersite quantal variability. Therefore, only the results for

intrasite quantal variability are summarized in Fig. 4. Considering the first pair of stimuli, it is seen that both decreasing q_1/q_0 and increasing M increase the negative correlation coefficient (Fig. 4 B). Regarding the covariance of the first pair of stimuli, it is seen that the absolute covariance is becoming larger when the quantal size is reduced moderately, whereas it falls again as the quantal size is strongly reduced (Fig. 4 A). The absolute values of both, covariance and correlation coefficient, decline along the stimulus train. In the variance–mean plot, the reduction in quantal size causes the late depressed responses in the train to deviate from the parabola, as shown in Fig. 4 C (inset). Figure 4 D shows that the number of release sites is underestimated when the covariance approach is applied to the first pair of stimuli, in agreement with Eq. 44 (e.g., for $M = 3$, $q_1/q_0 = 0.8$, and $p_0 = 0.5$, $D_{1,2}$ is 0.33, such that one expects $N_{cov} = 376$ compared to $N = 500$; Fig. 4 D, red trace). The absolute quantal size is overestimated by the covariance approach (Fig. 4 E, compare corresponding broken and solid lines) the more, the stronger the reduction by a single release event is (reducing q_1/q_0) or the more neighboring sites contribute. The correction factor $(1 - D_{i,i+1})$ (Eqs. 48 and 45, respectively) can be determined from the ratio of the correlation coefficients under equivalent recording conditions in the presence and absence of postsynaptic effects (Eq. 49). However, in case this information is not available, N_{cov} estimates are still useful, because D_{12} can be determined by comparing the prediction of Eq. 45 for the quantal size in the first response to the value obtained directly from recordings of mEPSCs. If, furthermore, $D_{i,i+1} = D = const$ and $D_{1,2}$ is known, Eq. 45 can still be used to calculate the quantal size for each response in a train. In the case of $M = 3$ and $q_1/q_0 = 80\%$ or $M = 20$ and $q_1/q_0 = 90\%$ variations in $(1 - D_{ij})$ are less than 40%. Nevertheless, even without such a correction, the relative changes in quantal size agree reasonably well with the values assumed in the simulation (Fig. 4 F, compare corresponding broken and solid lines), except for the case of $M = 3$ and $q_1/q_0 = 50\%$. This is again expected, since $D_{i,i+1}$ varies in the range between about -0.5 and 1.0 in this case.

DISCUSSION

We showed how the variance–mean approach to quantal analysis (Clamann et al., 1989; Silver et al., 1998; Reid and Clements, 1999; Oleskevich et al., 2000; Clements and Silver, 2000) can be extended to incorporate nonstationary responses from short stimulus trains to study synaptic plasticity. In addition, we introduced the analysis of the covariance between successive synaptic responses. We show that the combined analysis of mean, variance and covariance yields estimates for the quantal sizes q_i of individual responses i in a train. In addition, it yields estimates of the number of release sites N from a pair of stimuli, which are
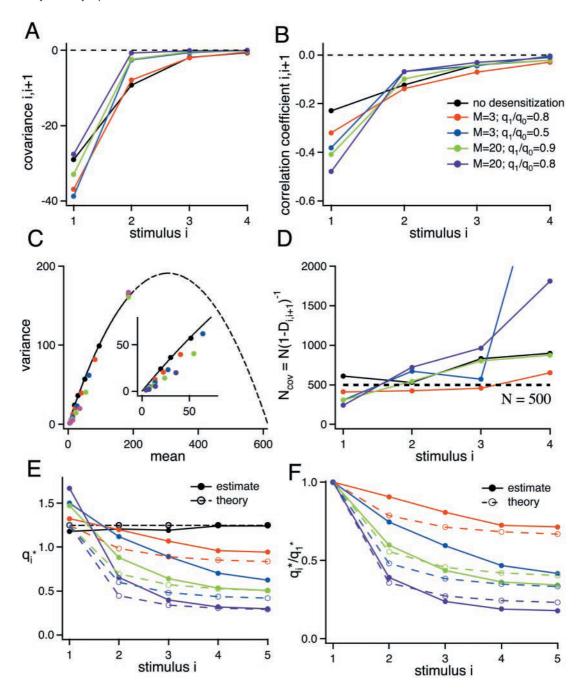
FIGURE 4 Summary of the results from simulations of trains of five stimuli assuming quantal size reduction. Simulations were performed for groups on $M = 3$ and 20 interacting release sites, with homogenous output probability of $p_0 = 0.5$ and different degrees of quantal size reduction. The latter parameter is given in the legend in panel B, which applies to the whole figure, as the quantal size ratio q_1/q_0 after a single release event. (A) Covariance between successive stimuli. (B) Correlation coefficient ($\rho_{i,i+1} \equiv \text{cov}_{i,i+1} \cdot (\text{var}_i \cdot \text{var}_{i+1})^{-1/2}$) between consecutive stimuli. (C) Variance–mean plots of the simulated data, the inset shows a blow-up of the low mean range. The parabola (*black line*) represents the case without desensitization. (D) Plot of the N estimate from the covariance versus stimulus number, which also shows whether $D_{i,i+1}$ is constant (refer to text for details). (E) Quantal size as estimated from the covariance approach according to Eq. 28 in comparison to the simulated (theoretical) quantal size. Note that the quantal size estimate of about 1.25 in the absence of desensitization (*black traces*) results from a mean quantal size of 1 and intrasite quantal size variability with CV = 0.5. (F) Data from part E replotted relative to the initial quantal size. All data are shown in arbitrary units with respect to a quantal size of 1 unit.

not affected by heterogeneity in the release probability under certain conditions.

In a number of studies, negative correlation between successive synaptic responses has been reported: At the neuromuscular junction (NMJ) (Elmquist and Quastel, 1964), at synapses of bipolar cells onto multipolar interneurons in the neocortex (Reyes et al., 1998), and at monosynaptic contacts of CA3 neurons onto CA1 or CA3 neurons in

the hippocampus (Thompson et al., 1998). Other synapses were shown not to display any correlation under the conditions tested. These include the connections of pyramidal cells onto bitufted gabaergic interneurons in the neocortex (Reyes et al., 1998) and Mauthner cell axons connecting onto cranial relay interneurons (Waldeck et al., 2000). However, so far, the covariance or correlation between successive responses has not yet been used for estimating synaptic parameters in practice, although this had been suggested by Vere-Jones (1966) and Quastel (1997). Both authors presented equivalent interpretations of the covariance between successive synaptic responses based on depletion of available neurotransmitter quanta. However, they did not provide explicit algorithms about how to determine any of the synaptic parameters from the covariance.

Our model predicts that the covariance between successive responses is always negative, and that its absolute value declines along a stimulus train (Fig. 4 *A*; Vere-Jones, 1966; Quastel, 1997). This was observed by Zucker (1973) at the NMJ. In contrast, Kraushaar and Jonas (2000) found correlation only in the late portion of trains at 20 Hz in the connection between dentate gyrus basket cells and granule cells in the hippocampus. Thus, for some synapses, alternative release models might be required to account for their transmission properties. The implications of the single-vesicle hypothesis (Korn et al., 1994) on the statistical parameters of synaptic transmission were studied by Matveev and Wang (2000). They considered the constraint that an active zone can release only one vesicle at a time, although more release-competent vesicles are available, and they concluded that the correlation between successive synaptic responses is negative for small vesicle fusion rates, but may become positive for larger rates. However, there has been no experimental evidence so far for positive correlation between successive synaptic responses. Still, the covariance analysis yields not only estimates of synaptic parameters, but can also help to distinguish between different models of synaptic transmission.

Interpretation of the variance–mean plot and the covariance approach in terms of synaptic plasticity

It can be expected that plastic changes of synaptic transmission result from a superposition of multiple cellular mechanisms acting simultaneously and in parallel (Zucker, 1989, 1999). Therefore, it is desirable to have approaches at hand that allow for quantification of any of the contributing mechanisms separately. The idea behind the concept of considering the release probability as the product of a probability of availability p_A and output probability p_0 by Vere-Jones (1966), Zucker (1989), Quastel (1997) was to introduce means, by which the depletion of available vesicles and any mechanism modulating the output probability, such as facilitation, can be determined separately. Our analysis

failed to provide any clues for separating p_A and p_0 by analysis of the variance and covariance in consecutive synaptic responses, because p_A and p_0 appear as product in all the equations derived here. The only solution to this problem seems to be the determination of the initial or resting availability p_A as the ratio of the total number of releasable quanta (as determined from a depleting train in the absence of pool refilling) over the number of release sites. In the variance mean plot, changes in the product of p_A and p_0, i.e., in the release probability, shift the data points along the variance mean parabola during a train of stimuli.

Changes in quantal size show up as deviations from the variance–mean parabola in the variance mean plot. The most likely causes for quantal size reductions are postsynaptic receptor saturation or desensitization towards the end of a short train. In that case, the late, depressed responses give rise to a reduced initial slope of the variance–mean plot with respect to a hypothetical parabola. In contrast to the variance–mean plot, the covariance approach allows quantification of the quantal size for each response in a train (Eq. 45), unless postsynaptic mechanisms introduce additional correlations (see below). For an accurate estimate of quantal size, knowledge of CV_q is required, which at many synapses can be obtained from a histogram of mEPSCs.

Once the quantal size has been determined, the quantal content can be calculated for each stimulus in a train from the ratio of EPSC amplitude over quantal size. Knowledge of the quantal content and its changes during repetitive stimulation allows study of presynaptic mechanisms of synaptic plasticity. Furthermore, information about the release probability can be obtained from the ratio of quantal content over number of release sites, as far as the latter is known.

The number of release sites N is a fixed parameter in the model and does not undergo transient changes. This should hold true in reality, too, as long as no fast recruitment of "silent" sites occurs. The duration of stimulus trains applied for studying short-term synaptic plasticity can be expected to be short compared to long-term processes involving protein synthesis to enhance the number of active presynaptic terminals (Ma et al., 1999). However, care must be taken that the repetitive application of short trains for obtaining the statistical data does not activate any long-term plasticity mechanisms, which might modify the number of release sites. N can either be determined from the width of the variance–mean plot, but this might severely underestimate the parameter in the presence of heterogeneity in the release probability. In contrast, the covariance approach yields an estimate for N, which is largely unaffected by heterogeneity in the release probability as long as its mean is around 0.5 (Fig. 2, *A* and *B*, *dotted line*). Because quantal size variability of the intersite type causes underestimation of N (Eqs. 18 and 48), knowledge of the CV_q of mEPSC amplitude variability, which might arise from both intra- and intersite quantal variability, can be used to obtain upper

and lower bounds for N as suggested by Frerking and Wilson (1996).

Estimates of the number of release sites N in the presence of heterogeneity in release probability

The estimation of the number of release sites from the mean and covariance of successive synaptic responses has the advantage over the conventional variance–mean analysis of being unaffected by heterogeneity in the release probability under the condition that the mean output probability is $\langle p_0 \rangle$ = 0.5 (Fig. 2). Heterogeneity in the release probability among or within release sites or active zones was reported by Walmsley et al. (1988), Rosenmund et al. (1993), Murthy et al. (1997), Silver et al. (1998), Wu and Borst (1999), and Sakaba and Neher (2001). It might arise from different priming states of docked vesicles (Xu et al., 1998), vesicles carrying variable amounts of synaptic proteins required for fusion (Littleton et al., 2001), differences in the relative localization of release sites and Ca^{2+} channels (Neher, 1998), and from variations in the number of docked and primed vesicles in case release sites are considered as active zones (Dobrunz and Stevens, 1997; Schikorski and Stevens, 1997).

For the conventional variance–mean analysis, Silver et al. (1998) provided a modification to estimate the degree of heterogeneity in the release probability by introducing a relationship between its mean and CV on the basis of a beta distribution. However, this requires sampling of the whole variance–mean parabola, which might not be possible for practical experimental reasons, and the assumption of a beta distribution is more or less arbitrary. Thus the approach described here should be quite valuable, if one succeeds in finding conditions in a given synaptic preparation, where at least two consecutive responses in a train reach a release probability of 0.5 or slightly larger. Our calculations and simulations show that, in this case, the error in the N estimate due to heterogeneity in the release probability hardly exceeds 20% (Fig. 2). The correctness of the assumption of $p_0 \approx 0.5$ can be examined in a consistency test a posteriori by calculating p_0 from the EPSC amplitudes.

Estimates of the number of release sites N and the quantal size q in the presence of correlation due to postsynaptic effects

It has been reported that, during repetitive synaptic activity, the apparent quantal size may be reduced due to saturation of postsynaptic receptors (Tong and Jahr, 1994), desensitization of postsynaptic receptors (Trussel et al., 1993; Otis et al., 1996b), or by incomplete neurotransmitter refilling of rapidly recycled vesicles (Behrends and Rumpel, 2000). Recording miniature EPSCs, Otis et al. (1996b) reported a reduction in quantal size by 54% within 50 ms after an

evoked EPSC, and Oleskevich et al. (2000) reported a reduction by 20% within 30 ms after a double pulse under the conditions tested. Furthermore, Oleskevich et al. (2000) applied the variance–mean analysis to double pulses recorded under different conditions in the rat endbulb of Held synapse to analyze paired-pulse depression. The data from the first pulse was in concord with the expected variance–mean parabola, whereas the data from the second pulses deviated from this parabola in a manner they referred to as curling back on itself for high release probabilities (see their Fig. 5). From simulations, they concluded that the observed deviation from the parabola, and therefore the paired pulse depression, is a mixture of pre- and postsynaptic mechanisms. However, this was not quantified further.

Although the application of the variance–mean approach presents problems, if the quantal size changes along a train of stimuli, such that a parabola cannot be fitted for determination of N and q (Fig. 4 C, *inset*), changes in quantal size during a train, as those caused by saturation and desensitization, can be readily measured by the covariance approach, as discussed above, unless they lead to additional correlation between responses within a train.

Quastel (1997) stated that any postsynaptic effects, such as postsynaptic receptor desensitization and saturation, increase the negative correlation between synaptic outputs. We analyzed this situation analytically and in Monte Carlo simulations. If additional correlations occur, our approach underestimates N and overestimates q as shown by Eqs. 48 and 45, respectively, and demonstrated by simulations (Fig. 4, D and E, comparing corresponding broken and solid lines). Although, for the estimation of N, the problem of postsynaptic effects, such as saturation and desensitization, can be avoided by application of drugs that prevent these effects (Diamond and Jahr, 1997; Yamada and Tang, 1993; Neher and Sakaba, 2001), analysis of the quantal size for each response in a train is desirable in the presence of postsynaptic effects to elucidate their contribution to short-term synaptic plasticity. To this end, our equations allow estimation of corrections that may have to be applied or else assignment of bounds to the expected errors. One possibility is to determine the correction factor from the ratio of the correlation coefficients under equivalent recording conditions in the presence and absence of postsynaptic effects (Eq. 49), obtained by application of appropriate drugs. In case this is not possible, but the correction factor is constant along the response train, it can be determined by comparing the estimated initial quantal size (Eq. 45) with the quantal size directly determined from recording of spontaneous synaptic events. Irrespective of whether the correction factor is constant, our simulation shows (Fig. 4 F, comparing corresponding broken and solid lines) that relative quantal size changes are predicted accurately within 20% except for extreme cases.

Estimates of the quantal size q and the number of release sites N in the presence of asynchronous release

All the arguments and simulations given above assumed perfect synchronization of release events during a presynaptic action potential. For a discussion of the N and q estimates with respect to possible asynchrony in release (Quastel, 1997), one has to distinguish two cases: a jitter of quantal release events around the time of the evoked current maximum, and release events that are so much delayed that they do not contribute to the evoked current peak at all. The jitter causes the quantal events to be sampled at different times along their time course, and, therefore, introduces some kind of artificial quantal size variability. Because this increases the variability in quantal size but at the same time decreases its mean, it may have only minor effects on the quantal-size estimate from analysis of the variance–mean plot or the covariance. Regarding the N estimate, however, the effect of such quantal variability depends on whether it is more equivalent to the intra- or the intersite type. If it would be of the intrasite type, it has no effect on the N estimate. This would be the case if the time dispersion of individual quantal events resulted, for example, from trial-to-trial variations in the Ca^{2+} concentration profile at a release site due to stochastic ion channel operation (Quastel, 1997). The intersite type, with an effect on the N estimate, would be present if the time dispersion resulted, for example, from differences in diffusional distance between release sites and Ca^{2+} channels (Borst and Sakmann, 1996).

Asynchrony in the release process can be accounted for by performing the analysis on the EPSC charge (time integral) instead of the peak amplitude (Bekkers and Stevens, 1995; Borst and Sakman 1996; Quastel, 1997). However, in the case of EPSC charge, a proper background subtraction, e.g., in the presence of a residual current (Neher and Sakaba, 2001), is more complicated compared to using the EPSC peak amplitude for quantification of transmitter release.

Practical approaches for estimating quantal parameters

Based on our theoretical analysis and the simulations presented, we suggest several alternatives as practical approaches to the analysis of synaptic transmission. If the aim is merely a distinction between changes in quantal content and quantal size during trains of stimuli under physiological conditions, we recommend judging the relative contribution of covariance to quantal size estimates (Eq. 45). This contribution may be substantial for the largest response in a train, but is probably small in later responses. Thus quantal size estimates for these late responses based on Eq. 45 should be correct.

For early, large responses, the quantal size may be overestimated by Eq. 45, because contributions to the covariance of postsynaptic origin should be of the same sign as those of vesicle depletion. The extent of such overestimation can be checked by comparing the estimates with a quantal size estimate obtained either from the mEPSC distribution or from an experiment performed under conditions where no saturation or desensitization is expected. Once reliable estimates of quantal size are obtained for each response in a train, one can calculate the quantal contents from the ratios of EPSC amplitudes over quantal sizes.

If the aim is to address the question of the number of release sites and heterogeneity in the release probability, it should be advisable to work under conditions, under which the contribution of postsynaptic effects on correlations can be neglected. An experiment as discussed above, should then provide the additional information about N and the mean release probabilities for individual responses. In any case, consideration of correlation within trains of responses should be helpful for a better dissection of pre- and postsynaptic effects associated with plastic changes in synaptic strength.

APPENDIX

Calculation of the signal-to-noise ratio of the segmented estimation of variance

In a stationary data set of size N, record n may be represented as the sum of its expectation independent of n and a fluctuating term with zero mean

$$x_n = x_0 + \delta x_n, \tag{A1}$$

with the expectation being the population mean,

$$E(x_n) = x_0, \tag{A2}$$

and variance being the variance of the population

$$V(x_n) = V(\delta x_n) = \sigma^2. \tag{A3}$$

Assuming the fluctuating term to be a Gaussian stochastic variable with zero mean in case that all δx_n and δx_m are statistically independent, the following equations hold (see Heinemann and Conti, 1992)

$$\langle \delta x_n \delta x_m \rangle = \langle \delta x_n \rangle \langle \delta x_m \rangle = 0; \quad m \neq n, \tag{A4}$$

$$\langle \delta x_n^2 \rangle = \sigma^2, \tag{A5}$$

$$\langle \delta x_n^2 \delta x_m^2 \rangle = \langle \delta x_n^2 \rangle \langle \delta x_m^2 \rangle = \sigma^4; \quad m \neq n, \tag{A6}$$

$$\langle \delta x_n^4 \rangle = 3\sigma^4. \tag{A7}$$

Mean and variance estimates are determined for a segment s of size R by

$$\bar{x}_s = \frac{1}{R} \sum_{n=n(s,R)}^{n(s,R)+R-1} x_n \tag{A8}$$

and

$$v_s = \frac{1}{R-1} \sum_{n=n(s,R)}^{n(s,R)+R-1} (x_n - \bar{x}_s)^2, \qquad (A9)$$

respectively, where $n(s, R)$ is the first entry of segment s.

The overall variance estimate is then given as the average segment variance,

$$v_{tot} = \langle v_s \rangle, \qquad (A10)$$

and the uncertainty in this estimate can be calculated by its variance as

$$\mathrm{Var}(v_{tot}) = \langle v_{tot}^2 \rangle - \langle v_{tot} \rangle^2. \qquad (A11)$$

Now the three different possibilities of choosing the segments with respect to their size and mutual overlap are examined regarding the uncertainty of the variance estimate they yield. These possibilities are nonoverlapping independent segments, that overlap by half the number of entries, and segments that are shifted along the entries of the data set in steps of one entry. Eq. A11 is analyzed for each case as a measure for the uncertainty of the variance estimate.

Nonoverlapping independent segments

Assume segments of size R and a data set of N records (note that N should be a multiple of R),

$$v_{tot} = \frac{1}{N/R} \sum_{s=1}^{N/R} v_s, \qquad (A12)$$

thus,

$$v_{tot}^2 = \frac{1}{(N/R)^2} \left[\sum_{s=1}^{N/R} v_s \right]^2, \qquad (A13)$$

and the expectations of Eqs. A12 and A13 are

$$\langle v_{tot} \rangle = \frac{1}{N/R} \sum_{i=s}^{N/R} \langle v_s \rangle = \langle v_s \rangle \qquad (A14)$$

and

$$\langle v_{tot}^2 \rangle = \frac{1}{(N/R)^2} \left[\sum_{s=1}^{N/R} \langle v_s^2 \rangle + 2 \sum_{s=1}^{N/R} \sum_{t=i+1}^{N/R} \underbrace{\langle v_s v_t \rangle}_{\text{non-overlapping}} \right]$$

which gives, with $\langle v_s v_t \rangle = \langle v_s \rangle \langle v_t \rangle = \langle v_s \rangle^2$, because nonoverlapping segments are independent,

$$\langle v_{tot}^2 \rangle = \frac{1}{N/R} \left[\langle v_s^2 \rangle + \left(\frac{N}{R} - 1 \right) \langle v_s \rangle^2 \right]. \qquad (A15)$$

Inserting Eqs. A13 and A15 into Eq. A11 yields

$$\mathrm{Var}(v_{tot}) = \frac{1}{N/R} \left(\langle v_s^2 \rangle - \langle v_s \rangle^2 \right). \qquad (A16)$$

Now, $\langle v_s \rangle$ and $\langle v_s^2 \rangle$ have to be determined. Substitution of Eqs. A1 and A8 into Eq. A9 and rearrangement yield

$$v_s = \frac{1}{R} \sum_{n=n(s,R)}^{n(s,R)+R-1} \delta x_n^2 - \frac{2}{R(R-1)} \sum_{n=n(s,R)}^{n(s,R)+R-1} \sum_{m=n+1}^{n(s,R)+R-1} \delta x_n \delta x_m.$$

$$(A17)$$

Calculation of $\langle v_s \rangle$, see Eqs. A4 and A5,

$$\langle v_s \rangle = \frac{1}{R} \sum_{n=n(s,R)}^{n(s,R)+R-1} \underbrace{\langle \delta x_n^2 \rangle}_{= \sigma^2}$$

$$- \frac{1}{R(R-1)} \sum_{n=n(s,R)}^{n(s,R)+R-1} \sum_{m=1, m\neq n}^{n(s,R)+R-1} \underbrace{\langle \delta x_n \delta x_m \rangle}_{= 0},$$

thus

$$\langle v_s \rangle = \sigma^2, \qquad (A18)$$

as expected. From Eq. A17 follows

$$v_s^2 = \frac{1}{R} \sum_{n=n(s,R)}^{n(s,R)+R-1} \sum_{m=n(s,R)}^{n(s,R)+R-1} \delta x_n^2 \delta x_m^2$$

$$- \frac{4}{R^2(R-1)} \sum_{n=n(s,R)}^{n(s,R)+R-1} \sum_{m=n(s,R)}^{n(s,R)+R-1} \sum_{l=m+1}^{n(s,R)+R-1} \delta x_n^2 \delta x_m \delta x_l$$

$$+ \frac{4}{R^2(R-1)^2} \left(\sum_{n=n(s,R)}^{n(s,R)+R-1} \sum_{m=n+1}^{n(s,R)+R-1} \delta x_n \delta x_m \right)^2. \quad (A19)$$

Calculating the expectation $\langle v_s^2 \rangle$, only the first and the last sum contribute nonzero terms, see Eqs. A4–A7:

$$\langle v_s^2 \rangle = \frac{1}{R^2} \sum_{n=i}^{s+R-1} \langle \delta x_n^4 \rangle$$

$$+ \frac{2}{R^2} \sum_{n=i}^{s+R-1} \sum_{m=n+1}^{s+R-1} \langle \delta x_n^2 \delta x_m^2 \rangle$$

$$+ \frac{4}{R^2(R-1)^2} \sum_{n=i}^{s+R-1} \sum_{m=n+1}^{s+R-1} \langle \delta x_n^2 \delta x_m^2 \rangle$$

$$= \frac{3}{R} \sigma^4 + \left(\frac{2}{R^2} + \frac{4}{R^2(R-1)^2} \right) \frac{R(R-1)}{2} \sigma^4,$$

and finally

$$\langle v_s^2 \rangle = \frac{R+1}{R-1} \sigma^4. \qquad (A20)$$

Substituting Eqs. A18 and A20 into Eq. A16 yields the uncertainty in the variance estimate for nonoverlapping segments of size R to be

$$\text{Var}(v_{\text{tot}}) = \frac{2R}{N(R-1)}\sigma^4. \tag{A21}$$

The results for $\langle v_s \rangle$ and $\langle v_s^2 \rangle$ (Eqs. A18 and A20) in this section hold generally for any data segment of size R.

Half-overlapping segments

Assume segments of size R and a data set of N records (note that N should be a multiple of R, R a multiple of 2),

$$v_{\text{tot}} = \frac{1}{(2N/R - 1)} \sum_{s=1}^{2N/R-1} v_s, \tag{A22}$$

and thus,

$$v_{\text{tot}}^2 = \frac{1}{(2N/R - 1)^2} \left[\sum_{s=1}^{2N/R-1} v_s^2 + 2 \sum_{s=1}^{2N/R-2} \underbrace{v_s v_{s+1}}_{\text{overlapping}} \right.$$

$$\left. + 2 \sum_{s=1}^{2N/R-1} \sum_{s=t+2}^{2N/R-1} \underbrace{v_s v_t}_{\text{non-overlapping}} \right]. \tag{A23}$$

The expectations of Eqs. A22 and A23 are

$$\langle v_{\text{tot}} \rangle = \langle v_s \rangle, \tag{A24}$$

as above in Eq. A18, and

$$\langle v_{\text{tot}}^2 \rangle = \frac{1}{2N/R - 1} \langle v_s^2 \rangle$$

$$+ \frac{4(N/R - 1)}{(2N/R - 1)^2} \underbrace{\langle v_s v_{s+1} \rangle}_{\text{half-overlapping}}$$

$$+ \frac{2(2N/R - 3)}{2N/R - 1} \underbrace{\langle v_s v_t \rangle}_{\substack{\text{non-overlapping} \\ = \langle v_s \rangle^2}}. \tag{A25}$$

Substituting Eqs. A24 and A25 into Eq. A11 yields

$$\text{Var}(v_{\text{tot}}) = \frac{1}{(2N/R - 1)} \langle v_s^2 \rangle + \frac{4(N/R - 1)}{(2N/R - 1)^2} \underbrace{\langle v_s v_{s+1} \rangle}_{\text{half-overlapping}}$$

$$+ \frac{6N/R - 5}{2N/R - 1} \langle v_s \rangle^2. \tag{A26}$$

Now we calculate $\langle v_i v_{i+1} \rangle$ for half-overlapping segments,

$$v_s = \frac{1}{R} \sum_{n=(R/2)(s-1)+1}^{(R/2)(s+1)} \delta x_n^2$$

$$- \frac{2}{R(R-1)} \sum_{n=(R/2)(s-1)+1}^{(R/2)(s+1)} \sum_{m=n+1}^{(R/2)(s+1)} \delta x_n \delta x_m. \tag{A27}$$

$R/2$ of the entries in the sums v_s and v_{s+1} occur in both. Calculating the expectation of the product of v_s and v_{s+1} only, the products of their first sums and their second sums contribute nonzero terms (see Eqs. A4–A7),

$$\langle v_s v_{s+1} \rangle = \frac{1}{R^2}\left[\frac{R}{2\langle \delta x_n^4 \rangle} + \frac{R}{2(R-1)\langle \delta x_n^2 \delta x_m^2 \rangle} + \frac{R^2}{2\langle \delta x_n^2 \delta x_m^2 \rangle} \right]$$

$$+ \frac{4}{R^2(R-1)^2}\left[\frac{R}{4(R/2-1)\langle \delta x_n^2 \delta x_m^2 \rangle} \right] \quad n \neq m. \tag{A28}$$

This gives, with Eqs. A6 and A7,

$$\langle v_s v_{s+1} \rangle = \left[1 + \frac{1}{R} + \frac{R/2 - 1}{R(R-1)^2} \right]\sigma^4. \tag{A29}$$

Thus, finally, by insertion of Eqs. A18, A20, and A28 into Eq. A26,

$$\text{Var}(v_{\text{tot}}) = \left[\frac{(R+1)}{(2N/R - 1)(R-1)} \right.$$

$$+ 4\frac{(N/R - 1)}{(2N/R - 1)^2}\left(1 + \frac{1}{R} + \frac{(R/2 - 1)}{R(R-1)^2} \right)$$

$$\left. - \frac{(6N/R - 5)}{(2N/R - 1)} \right]\sigma^4. \tag{A30}$$

Completely overlapping segments

Assume segments of size R and a data set of N records

$$v_{\text{tot}} = \frac{1}{(N - R + 1)} \sum_{s=1}^{N-R+1} v_s, \tag{A31}$$

$$v_{\text{tot}}^2 = \frac{1}{(N - R + 1)^2}\left[\sum_{s=1}^{N-R+1} v_s^2 + 2\sum_{s=1}^{N-R+1}\sum_{t=s+1}^{N-R+1} v_s v_t \right]. \tag{A32}$$

The expectation of Eq. A31 is

$$\langle v_{\text{tot}} \rangle = \langle v_s \rangle. \tag{A33}$$

For the expectation $\langle v_{\text{tot}}^2 \rangle$ of Eq. A33, two cases must be distinguished:
1) All segments overlap with any other if $R \geq (N+1)/2$ (first segment ends at $n_{\text{end}} = R$, last segment starts at $n_{\text{start}} = N - R + 1$),

$$v_{\text{tot}}^2 = \frac{1}{(N - R + 1)^2}\left[\sum_{s=1}^{N-R+1} v_s^2 + 2\sum_{s=1}^{N-R+1}\sum_{t=1}^{N-R} \underbrace{v_s v_{s+t}}_{\text{overlapping}} \right], \tag{A34}$$

such that

$$\langle v_{\text{tot}}^2 \rangle = \frac{1}{(N - R + 1)} \langle v_s^2 \rangle$$

$$+ 2\sum_{s=1}^{N-R} \frac{(N - R + 1 - t)}{(N - R + 1)^2} \langle v_s v_{s+t} \rangle. \tag{A35}$$

2) Not all segments overlap with any other in case $R < (N + 1)/2$,

$$v_{tot}^2 = \frac{1}{(N - R + 1)^2} \left[\sum_{s=1}^{N-R+1} v_s^2 + \sum_{s=1}^{N-R+1} \sum_{t=1}^{R-1} \underbrace{v_s v_{s+t}}_{\text{overlapping}} \right.$$

$$\left. + \sum_{s=1}^{N-R+1} \sum_{t=R}^{N-R} \underbrace{v_s v_{s+t}}_{\substack{\text{non-overlapping} \\ = \langle v_s \rangle^2}} \right], \quad (A36)$$

such that

$$\langle v_{tot}^2 \rangle = \frac{1}{(N - R + 1)^2} \langle v_s^2 \rangle$$

$$+ 2 \sum_{t=1}^{R-1} \frac{(N - R + 1 - t)}{(N - R + 1)^2} \langle v_s v_{s+t} \rangle$$

$$+ \frac{(N - 2R + 1)(N - 2R + 2)}{(N - R + 1)^2} \langle v_s \rangle^2. \quad (A37)$$

Now we calculate $\langle v_s v_{s+t} \rangle$,

$$v_s = \frac{1}{R} \sum_{n=s}^{s+R-1} \delta x_n^2 - \frac{2}{R(R-1)} \sum_{n=s}^{s+R-1} \sum_{m=n+1}^{s+R-1} \delta x_n \delta x_m, \quad (A38)$$

and define the number of entries contained in both v_s and v_{s+t}, which is

$$X_t \equiv R - t. \quad (A39)$$

As in the above sections, again, only the products of the first sum of v_s with the first sum of v_{s+t} and the second sum of v_s with the second sum of v_{s+t} yield nonzero terms for the expectation, such that

$$\langle v_s v_{s+t} \rangle = \frac{1}{R^2} [X_t \langle \delta x_n^4 \rangle + X_t (R - 1) \langle \delta x_n^2 \delta x_m^2 \rangle$$

$$+ (R - X_t) R \langle \delta x_n^2 \delta x_m^2 \rangle]$$

$$+ \frac{4}{R^2 (R - 1)^2} [X_t (X_t - 1)/2 \langle \delta x_n^2 \delta x_m^2 \rangle] \quad n \neq m.$$

After rearrangement and insertion of Eq. A39, this gives

$$\langle v_s v_{s+t} \rangle = \left[1 + \frac{2}{R} - \frac{2t}{R^2} + 2 \frac{(R - t)(R - t - 1)}{R^2 (R - 1)^2} \right] \sigma^4. \quad (A40)$$

Now all expressions required for insertion into Eq. 11 are derived (Eqs. A6, A7, A18, A20, A35, A37, and A40), to get the variance of the variance estimate in the two cases of totally overlapping segments. The analytical expressions for Var(v_{tot}) are quite long, and therefore not explicitly given here.

Comparing the three possibilities of overlap, one finds that, in each case the variance of the variance estimate can be written as a product of the fourth power of the intrinsic standard deviation σ and a factor that depends on the size of the data set N, the segment size R, and the method of choice

x (see Eqs. A21 and A30 for the third case, the explicit expression is not given):

$$\text{Var}(v_{tot}) = \text{factor}_x(N, R) \sigma^4. \quad (A41)$$

From Eq. A41, it follows for the signal-to-noise ratio of the total variance estimate,

$$\text{SNR}(v_{tot}) = \frac{\langle v_{tot} \rangle}{\sqrt{\text{Var}(v_{tot})}} = \frac{1}{\sqrt{\text{factor}_x(N, R)}}. \quad (A42)$$

This is plotted in the Fig. 1 E for the three possibilities over a range of segment sizes at a fixed data-set size of $N = 100$.

Calculation of the uncertainty of the segmented estimation of the covariance

Assume a data set containing N recorded trains. The calculation is carried out analogous to the calculation for the uncertainty in the variance, with the difference that, here, only the cases of independent records and the segmental estimation with overlapping windows of size 2 are considered. For records x_{ni} and x_{ni+1} of two successive responses i and $i + 1$ in train n, we can write in analogy to Eqs. A1, A2, and A3,

$$x_{ni} = x_{0i} + \delta x_{ni}$$

with

$$\langle x_{ni} \rangle = x_{0i}, \quad \langle \delta x_{ni} \rangle = 0, \quad \text{Var}(x_{ni}) = \text{Var}(\delta x_{ni}) = \sigma_i^2,$$
$$(A43)$$

$$x_{ni+1} = x_{0i+1} + \delta x_{ni+1}$$

with

$$\langle x_{ni+1} \rangle = x_{0i+1}, \quad \langle \delta x_{ni+1} \rangle = 0,$$

$$\text{Var}(x_{ni+1}) = \text{Var}(\delta x_{ni+1}) = \sigma_{i+1}^2, \quad (A44)$$

The fluctuations δx_{ni} and δx_{nj} are assumed not to be independent for $i = j$, but each is distributed in a Gaussian fashion, such that Eqs. A4–A7 hold here, too.

N independent records

In the case of N independent records, the equation for the covariance estimation is

$$\text{cov}_{i,i+1} = \frac{1}{(N-1)} \sum_{n=1}^{N} (x_{ni} - \bar{x}_i)(x_{ni+1} - \bar{x}_{i+1}), \quad (A45)$$

with

$$\bar{x}_i = \frac{1}{N} \sum_{n=1}^{N} x_{ni} \quad \text{and} \quad \bar{x}_{i+1} = \frac{1}{N} \sum_{n=1}^{N} x_{ni+1}. \quad (A46)$$

The expected value of the covariance estimate is

$$\langle \text{cov}_{i,i+1} \rangle = \langle \delta x_i \delta x_{i+1} \rangle. \quad (A47)$$

The expected value of the squared covariance estimate is

$$\langle \text{cov}_{i,i+1}^2 \rangle = \frac{1}{N} \langle \delta x_i^2 \delta x_{i+1}^2 \rangle + \frac{N-1}{N} \langle \delta x_i \delta x_{i+1} \rangle^2. \quad \text{(A48)}$$

The variance of the covariance estimation is

$$\text{Var}(\text{cov}_{i,i+1}) = \langle \text{cov}_{i,i+1}^2 \rangle - \langle \text{cov}_{i,i+1} \rangle^2. \quad \text{(A49)}$$

With insertion of Eqs. A47 and A48 into Eq. A49, the variance of the covariance estimation is

$$\text{Var}(\text{cov}_{i,i+1}) = \frac{1}{N} (\langle \delta x_i^2 \delta x_{i+1}^2 \rangle - \langle \delta x_i \delta x_{i+1} \rangle^2). \quad \text{(A50)}$$

Upper bounds of the terms in Eq. A50 are on the basis of σ_i, σ_{i+1} and the Schwarz inequality (see Bronstein and Semendjajew, 1989)

$$\langle \delta x_i \delta x_{i+1} \rangle^2 \leq \sigma_i^2 \sigma_{i+1}^2 \quad \text{(A51)}$$

and

$$\langle \delta x_i^2 \delta x_{i+1}^2 \rangle \leq 3\sigma_i^2 \sigma_{i+1}^2. \quad \text{(A52)}$$

Substituting Eqs. A51 and A52 into Eq. A50 yields an upper bound for the variance of the estimate of the covariance from N independent records,

$$\text{Var}(\text{cov}_{i,i+1}) \leq \frac{3}{N} \sigma_i^2 \sigma_{i+1}^2. \quad \text{(A53)}$$

N records analyzed segment-wise with overlapping segments of size R = 2

In the case of N records analyzed segment-wise with overlapping segments of size $R = 2$, the formula for the covariance estimation is

$$\text{cov}_{i,i+1} = \frac{1}{(N-1)} \sum_{s=1}^{N-1} \text{cov}_s, \quad \text{(A54)}$$

with

$$\text{cov}_s = \sum_{n=s}^{s+1} (x_{ni} - \bar{x}_{si})(x_{ni+1} - \bar{x}_{si+1}) \quad \text{(A55)}$$

and

$$\bar{x}_s = \frac{1}{2} \sum_{n=s}^{s+1} x_{ni} \quad \text{and} \quad \bar{x}_{si+1} = \frac{1}{2} \sum_{n=s}^{s+1} x_{ni+1}. \quad \text{(A56)}$$

Inserting Eq. A56 into Eq. A55 gives

$$\text{cov}_s = \frac{1}{2} (\delta x_{ni} - \delta x_{n+1i})(\delta x_{ni+1} - \delta x_{n+1i+1}). \quad \text{(A57)}$$

The uncertainty in the estimate of the covariance expressed as the variance of the estimate is

$$\text{Var}(\text{cov}_{i,i+1}) = \langle \text{cov}_{i,i+1}^2 \rangle - \langle \text{cov}_{i,i+1} \rangle^2. \quad \text{(A58)}$$

The expectation of Eq. A54 is again

$$\langle \text{cov}_{i,i+1} \rangle = \langle \text{cov}_s \rangle = \langle \delta x_i \delta x_{i+1} \rangle. \quad \text{(A59)}$$

The square of Eq. A54 is

$$\text{cov}_{i,i+1}^2 = \frac{1}{(N-1)^2} \left[\sum_{s=1}^{N-1} \text{cov}_s^2 + \sum_{s=1}^{N-1} \text{cov}_s \text{cov}_{s+1} \right. $$
$$\left. + 2 \sum_{s=1}^{N-1} \sum_{t=s+2}^{N-1} \text{cov}_s \text{cov}_t \right]. \quad \text{(A60)}$$

The expectation of Eq. A60 is

$$\langle \text{cov}_{i,i+1}^2 \rangle = \frac{(N-1)\langle \text{cov}_s^2 \rangle + 2(N-2)\langle \text{cov}_s \text{cov}_{s+1} \rangle + (N-2)(N-3)\langle \text{cov}_s \rangle^2}{(N-1)^2}. \quad \text{(A61)}$$

The expectation of the square of Eq. A57 is

$$\langle \text{cov}_s^2 \rangle = \frac{1}{2} (\langle \delta x_{ni}^2 \delta x_{ni+1}^2 \rangle + 2\langle \delta x_{ni} \delta x_{ni+1} \rangle^2 + \langle \delta x_{ni}^2 \rangle \langle \delta x_{ni+1}^2 \rangle. \quad \text{(A62)}$$

The expectation of the product of the covariance estimates of two successive segments is

$$\langle \text{cov}_s \text{cov}_{s+1} \rangle = \frac{1}{4} (\langle \delta x_{ni}^2 \delta x_{ni+1}^2 \rangle + 3\langle \delta x_{ni} \delta x_{ni+1} \rangle^2). \quad \text{(A63)}$$

Insertion of Eqs. A59 and A61 and, further, Eq. A62 and A63 into A58 gives the variance of the covariance estimation as

$$\text{Var}(\text{cov}_{i,i+1}) = \frac{1}{2(N-1)} \langle \delta x_{ni}^2 \rangle \langle \delta x_{ni+1}^2 \rangle$$
$$+ \frac{2N-3}{2(N-1)^2} \langle \delta x_{ni}^2 \delta x_{ni+1}^2 \rangle$$
$$+ \frac{2-N}{2(N-1)^2} \langle \delta x_{ni} \delta x_{ni+1} \rangle^2. \quad \text{(A64)}$$

The estimation of upper and lower bounds for this expression, based on σ_i, σ_{i+1} as above for $N > 2$ (note that the third term is negative) yields, for large values of N,

$$0 \leq \text{Var}(\text{cov}_{i,i+1}) \leq \frac{7N-10}{2(N-1)^2} \sigma_i^2 \sigma_{i+1}^2 \approx \frac{3.5}{N} \sigma_i^2 \sigma_{i+1}^2 \quad \text{(A65)}$$

REFERENCES

Barbour, B., and M. Hausser. 1997. Intersynaptic diffusion of neurotransmitter. *Trends Neurosci.* 20:377–384.

Bekkers, J. M., and C. F. Stevens. 1995. Quantal analysis of EPSCs recorded from small numbers of synapses in hippocampal cultures. *J. Neurophysiol.* 73:1145–1156.

Behrends, J. C., and E. Rumpel. 2000. Inhibitors of vesicle filling selectively affect high frequency transmission at striatal gabanergic synapses in vitro. *Eur. Biophys. J.* 29:349 (abstract).

Borst, J. G., and B. Sakmann. 1996. Calcium influx and transmitter release in a fast CNS synapse. *Nature.* 383:431–434.

Bronstein, I. N., and K. A. Semendjajew. 1989. Taschenbuch der Mathematik. BSB B. G. Teubner Verlagsgesellschaft, Leipzig, Germany. 240.

Clamann, H. P., J. Mathis, and H. R. Luscher. 1989. Variance analysis of excitatory postsynaptic potentials in cat spinal motoneurons during posttetanic potentiation. *J. Neurophysiol.* 61:403–416.

Clements, J. D., and R. A. Silver. 2000. Unveiling synaptic plasticity: a new graphical and analytical approach. *Trends Neurosci.* 23:105–113.

Del Castillo, J., and B. Katz. 1954. Quantal components of the endplate potential. *J. Physiol.* 124:560–573.

Diamond, J. S., and C. E. Jahr. 1997. Transporters buffer synaptically released glutamate on a submillisecond time scale. *J. Neurosci.* 17: 4672–4687.

Dobrunz, L. E., and C. F. Stevens. 1997. Heterogeneity of release probability, facilitation, and depletion at central synapses. *Neuron.* 18: 995–1008.

Elmquist, D., and D. M. J. Quastel. 1964. A quantitative study of the end-plate potentials in isolated human muscle. *J. Physiol.* 178:505–529.

Frerking, M., and M. Wilson. 1996. Effects of variance in mini amplitude on stimulus-evoked release: a comparison of two models. *Biophys. J.* 70:2078–2091.

Heinemann, S. H., and F. Conti. 1992. Nonstationary noise analysis and application to patch clamp recordings. *Methods Enzymol.* 207:131–148.

Korn, H., A. Mallet, A. Triller, and D. S. Faber. 1982. Transmission at a central inhibitory synapse. II. Quantal description of release, with a physical correlate for binomial *n*. *J. Neurophysiol.* 48:679–707.

Korn, H., C. Sur, S. Charpier, P. Legendre, and D. S. Faber. 1994. The one-vesicle hypothesis and multivesicular release. *In* Molecular and Cellular Mechanisms of Neurotransmitter Release. L. Stjärne, P. Greengard, G. S., T. Hökfelt, and D. Ottoson, editors. Raven Press Ltd., New York. 301–322.

Kraushaar, U., and P. Jonas. 2000. Efficacy and stability of quantal GABA release at a hippocampal interneuron-principal neuron synapse. *J. Neurosci.* 20:5594–5607.

Littleton, J. T., J. Bai, B. Vyas, R. Desai, A. E. Baltus, M. B. Garment, S. D. Carlson, B. Ganetzky, and E. R. Chapman. 2001. Synaptotagmin mutants reveal essential functions for the C2B domain in Ca^{2+}-triggered fusion and recycling of synaptic vesicles in vivo. *J. Neurosci.* 21:1421–1433.

Ma, L., L. Zablow, E. R. Kandel, and S. A. Siegelbaum. 1999. Cyclic AMP induces functional presynaptic boutons in hippocampal CA3-CA1 neuronal cultures [see comments]. *Nature Neurosci.* 2:24–30.

Matveev, V., and X. J. Wang. 2000. Implications of all-or-none synaptic transmission and short-term depression beyond vesicle depletion: a computational study. *J. Neurosci.* 20:1575–1588.

McLachlan, E. M. 1978. The statistics of transmitter release at chemical synapses. *Int. Rev. Physiol. Neurophysiol.* 3:49–117.

Meyer, A. 1999. Untersuchungen zur Wahrscheinlichkeit der Transmitterfreisetzung an einer zentralen Synapse. Diploma. Georg-August-University, Göttingen, Germany.

Murthy, V. N., T. J. Sejnowski, and C. F. Stevens. 1997. Heterogeneous release properties of visualized individual hippocampal synapses. *Neuron.* 18:599–612.

Neher, E. 1998. Vesicle pools and Ca^{2+} microdomains: new tools for understanding their roles in neurotransmitter release. *Neuron.* 20:389–399.

Neher, E., and T. Sakaba. 2001. Combining deconvolution and noise analysis for the estimation of transmitter release rates at the Calyx of Held. *J. Neurosci.* 21:444–461.

Oleskevich, S., J. Clements, and B. Walmsley. 2000. Release probability modulates short-term plasticity at a rat giant terminal. *J. Physiol.* 524:513–523.

Orear, J. 1982. Least squares when both variables have uncertainties. *Am. J. Phys.* 50:912–916.

Otis, T. S., Y. C. Wu, and L. O. Trussell. 1996a. Delayed clearance of transmitter and the role of glutamate transporters at synapses with multiple release sites. *J. Neurosci.* 16:1634–1644.

Otis, T., S. Zhang, and L. O. Trussell. 1996b. Direct measurement of AMPA receptor desensitization induced by glutamatergic synaptic transmission. *J. Neurosci.* 16:7496–7504.

Quastel, D. M. 1997. The binomial model in fluctuation analysis of quantal neurotransmitter release. *Biophys. J.* 72:728–753.

Redman, S. 1990. Quantal analysis of synaptic potentials in neurons of the central nervous system. *Physiol. Rev.* 70:165–198.

Reid, C. A., and J. D. Clements. 1999. Postsynaptic expression of long-term potentiation in the rat dentate gyrus demonstrated by variance–mean analysis. *J. Physiol.* 518:121–130.

Reyes, A., R. Lujan, A. Rozov, N. Burnashev, P. Somogyi, and B. Sakmann. 1998. Target-cell-specific facilitation and depression in neocortical circuits. *Nat. Neurosci.* 1:279–285.

Rosenmund, C., J. D. Clements, and G. L. Westbrook. 1993. Nonuniform probability of glutamate release at a hippocampal synapse. *Science.* 262:754–757.

Sakaba, T., and E. Neher. 2001. Quantitative relationship between transmitter release and calcium current at the Calyx of Held synapse. *J. Neurosci.* 21:462–476.

Schikorski, T., and C. F. Stevens. 1997. Quantitative ultrastructural analysis of hippocampal excitatory synapses. *J. Neurosci.* 17:5858–5867.

Sigworth, F. J. 1980. The variance of sodium current fluctuations at the node of Ranvier. *J. Physiol.* 307:97–129.

Silver, R. A., A. Momiyama, and S. G. Cull-Candy. 1998. Locus of frequency-dependent depression identified with multiple-probability fluctuation analysis at rat climbing fibre-Purkinje cell synapses. *J. Physiol.* 510:881–902.

Thompson, S. M., D. Debanne, and M. Capogna. 1998. Presynaptic determinants of synaptic efficacy in hippocampal pyramidal neurons. *In* Central Synapses: Quantal Mechanisms and Plasticity. D. S. Faber, H. Korn, S. J. Redman, S. M. Thompson, and J. S. Altman, editors. Human Frontier Science Program, Strasbourg, France. 247–254.

Tong, G., and C. E. Jahr. 1994. Multivesicular release from excitatory synapses of cultured hippocampal neurons. *Neuron.* 12:51–59.

Trussell, L. O., S. Zhang, and I. M. Raman. 1993. Desensitization of AMPA receptors upon multiquantal neurotransmitter release. *Neuron.* 10:1185–1196.

Vere-Jones, D. 1966. Simple stochastic models for the release of quanta of transmitter from a nerve terminal. *Austr. J. Statistics.* 8:53–63.

von Gersdorff, H., R. Schneggenburger, S. Weis, and E. Neher. 1997. Presynaptic depression at a calyx synapse: the small contribution of metabotropic glutamate receptors. *J. Neurosci.* 17:8137–8146.

Waldeck, R. F., A. Pereda, and D. S. Faber. 2000. Properties and plasticity of paired-pulse depression at a central synapse. *J. Neurosci.* 20:5312–5320.

Walmsley, B. 1993. Quantal analysis of synaptic transmission. *In* Electrophysiology. D. I. Wallis, editor. Oxford University Press, Oxford/New York/Tokyo. 109–141.

Walmsley, B., F. R. Edwards, and D. J. Tracey. 1988. Nonuniform release probabilities underlie quantal synaptic transmission at a mammalian excitatory central synapse. *J. Neurophys.* 60:889–908.

Weis, S., R. Schneggenburger, and E. Neher. 1999. Properties of a model of Ca^{2+}-dependent vesicle pool dynamics and short term synaptic depression. *Biophys. J.* 77:2418–2429.

Wu, L. G., and J. G. Borst. 1999. The reduced release probability of releasable vesicles during recovery from short-term synaptic depression. *Neuron.* 23:821–832.

Xu, T., T. Binz, H. Niemann, and E. Neher. 1998. Multiple kinetic components of exocytosis distinguished by neurotoxin sensitivity. *Nat. Neurosci.* 1:192–200.

Yamada, K. A., and C. M. Tang. 1993. Benzothiadiazides inhibit rapid glutamate receptor desensitization and enhance glutamatergic synaptic currents. *J. Neurosci.* 13:3904–3915.

Zucker, R. S. 1973. Changes in the statistics of transmitter release during facilitation. *J. Physiol.* 229:787–810.

Zucker, R. S. 1989. Short-term synaptic plasticity. *Ann. Rev. Neurosci.* 12:13–31.

Zucker, R. S. 1999. Calcium- and activity-dependent synaptic plasticity. *Curr. Opin. Neurobiol.* 9:305–313.